Understanding changes in the water budget driven by climate change in cryospheric-dominated watershed of the northeast Tibetan Plateau, China

Min Xu [1, 2], Shichang Kang [1, 3]*, Xiaoming Wang [1], Nick Pepin [4], Hao Wu [5]

[1]State Key Laboratory of Cryospheric Science, Northwest Institute of Eco-Environment and Resources, Chinese Academy of Sciences, Lanzhou, 730000, China

[2]Faculty of Geo-Information Science and Earth Observation, University of Twente, Enschede, 7513BH, Netherlands

[3]CAS Center for Excellence in Tibetan Plateau Earth Sciences, Chinese Academy of Sciences, Beijing, 100101, China

[4]Department of Geography, University of Portsmouth, Portsmouth, UK

[5]State Key Laboratory of Water Resources and Hydropower Engineering Science, Wuhan University, Wuhan, 430072, China

* Corresponding to Shichang Kang (shichang.kang@lzb.ac.cn)

This article has been accepted for publication and undergone full peer review but has not been through the copyediting, typesetting, pagination and proofreading process which may lead to differences between this version and the Version of Record. Please cite this article as doi: 10.1002/hyp.13383

Abstract: Glacial retreat and the thawing of permafrost due to climate warming have altered the hydrological cycle in cryospheric-dominated watersheds. In this study, we analysed the impacts of climate change on the water budget for the upstream of Shule River Basin on the northeast Tibetan Plateau. The results showed that temperature and precipitation increased significantly during 1957-2010 in study area. The hydrological cycle in the study area has intensified and accelerated under recent climate change. The average increasing rate of discharge in the upstream of Shule River Basin was 7.9 $\times 10^6$ m^3 /year during 1957-2010. As the mean annual glacier mass balance lost -62.4 mm/year, the impact of glacier discharge on river flow has increased, especially after 2000s. The contribution of glacier melt to discharge was approximately 187.99$\times 10^8$ m^3 or 33.4% of the total discharge over the study period. The results suggested that the impact of warming overcome the effect of precipitation increase on runoff increase during study period. The evapotranspiration (ET) increased during 1957-2010 with a rate of 13.4 mm /10 years. Based on water balance and GRACE and GLDAS data, the total water storage change showed a decreasing trend, whereas groundwater increased dramatically after 2006. As permafrost has degraded under climate warming, surface water can infiltrate deep into the ground, thus changing both the watershed storage and the mechanisms of discharge generation. Both the change in terrestrial water storage and changes in groundwater have had a strong control on surface discharge in the upstream of Shule River Basin. Future trends in runoff are forecasted based on climate scenarios. It is suggested that the impact of warming will overcome the effect of precipitation increase on runoff in the study area. Further studies such as this will improve understanding of water balance in cold high-elevation regions.

Keywords: Tibetan Plateau; water budget; climate change; cryosphere; effect

1. Introduction

The Tibetan Plateau, also called the "Asian Water Tower", is the highest and most extensive plateau in the world. It has an area of approximately 250×10^4 km^2 and an average elevation of more than 4000 m a.s.l. The cryosphere in China is primarily located on the Tibetan Plateau and more than one-sixth of the global population is influenced by glacier and snow melt water (Immerzeel *et al*., 2010; Sorg *et al*., 2014). Investigations have showed that there are 36763 glaciers with a total area of 49 873.44 km^2 on the Tibetan Plateau, and the area of permafrost is about 126×10^4 km^2 (Liu *et al*., 1995, Yao *et al*., 2013). Because of the shrinking cryosphere over the past decades (Wu and Zhang, 2008; Liu et al, 2006, Kang et al. 2010, 2015; Yao et al, 2012). the Tibetan Plateau is considered to be one of the most sensitive indicators of climate change in China (Yang, *et al*., 2011). Changes in temperature and precipitation over past decades were expected to significantly affect the cryospheric balances and the hydrology of headwater catchments on the Tibetan Plateau (Yang, *et al*., 2011; Duethmann, *et al*., 2014; Zhang *et al*., 2016; Gao *et al*., 2016, 2017). Therefore, systematic understanding of implications for the water budget in cryospheric watersheds is a key issue. It is not only helpful for understanding the response of the Tibetan Plateau hydrological cycle to climate change, but also benefits for water resource management in alpine regions.

The components of the water budget on the watershed include precipitation, discharge, evaporation and water storage change including changes in snow water equivalent, soil water and groundwater (Fig. 1). Previous studies indicated that ground meteorological observations showed distinct warming (>2.0 ℃) over Tibetan Plateau during the last half century, while precipitation did not change much over the same period (Yang *et al*., 2014). The watersheds on Tibetan Plateau also include glaciers and permafrost which are particularly sensitive to climate change. Since the 1990s the majority of glaciers have retreated rapidly and glacier mass loss has been dramatic with primary impact on the discharge of glacier-fed rivers (Yao *et al*., 2004, 2012; Bolch *et al*,. 2012, Gao *et al*., 2012). Barnett et al. (2005) indicated that vanishing glaciers would reduce water supply in the glaciated regions of the Tibetan Plateau. However, Su et al. (2016) indicated that the contribution of meltwater to discharge of major rivers differs fundamentally under different precipitation regimes on the Tibetan Plateau. In the upper Brahmaputra for example, the total discharge would increase by 2.7-22.4% in the long term due to a combination of increased rainfall-induced discharge and increased glacier melt, and more than 50% of the total discharge increase is attributed to the

increased glacier melt in the long run in the upper Brahmaputra. Therefore, glacier mass balance and glacier discharge both significantly affect catchment hydrology by temporarily storing and releasing water on various time scales.

Permafrost is also sensitive to the global climatic change (Wang *et al*., 2009; Ye *et al*., 2009). The Tibetan Plateau is the only region of the world where permafrost exists in the mid-latitudes. Previous studies have indicated that thawing in areas with an active layer depth of up to 60 cm contributed to an increase in discharge, however, once the active layer has increased beyond 60 cm, any more thawing led to a decrease in surface runoff and made the recession process slowly (Wang *et al*., 2009). The supra-permafrost groundwater discharge decreases exponentially with active layer frozen processes during the autumn period when runoff recedes, whereas the ratio of groundwater discharge to total discharge and the direct surface discharge coefficient simultaneously increase (Wang *et al*., 2012, 2017). As a special regional aquitard, permafrost obstructs or significantly weakens the spatiotemporal hydraulic connection between groundwater and surface water, it plays a decisive role in the formation of cold groundwater, transport processes, and the pattern of distribution of groundwater and its pathways (Zhang *et al*., 2008; Gao *et al*., 2016; Niu *et al*., 2016; Qin *et al*., 2017). Therefore, permafrost has significant effects on surface discharge, soil water content and the groundwater contribution which together induced the significant changes in the water budget.

Evaporation is also a critical process that determines the terrestrial water budget and water cycle. It is however, one of the most difficult components in the hydrological cycle to measure. Many regional studies have demonstrated that different measures of evaporation have showed different changes (Lawrimore and Peterson; Hobbins *et al*., 2004). Some studies just focused on potential evapotranspiration (or pan evaporation) on the Tibetan Plateau (Zhang *et al*., 2007; Liu *et al*., 2011). Only recently a number of estimates based on the Penman-Monteith method have become available on the Tibetan Plateau (Chen *et al*., 2006; Yang *et al*., 2011; Zhang *et al*., 2016). In summary, the climate change has lead to rapid changes in the cryospheric environment during recent decades on the Tibetan Plateau. Changes in glacier mass balance, thickening of the active layer and increasing permafrost temperature all influenced the water budget on the Tibetan Plateau (Kang *et al*., 2010; Wang *et al*., 2012; Yao *et al*,, 2012; Niu *et al*., 2016). However, most hydrological studies have focused solely on trends of individual hydro-meteorological

parameters. Detailed investigations of changes in a specific watershed including precipitation, discharge, evaporation, soil water content and groundwater in the context of changes in glacier mass balance and permafrost have seldom been discussed. This might be because of the many difficulties in the estimation of each component of the water budget in cold and high altitude regions.

In this study, different components of the water budget were estimated using a variety of methods in a cryospheric-dominated watershed of the northeast Tibetan Plateau. The contents of research include (1) The changes of components of water balance were calculated by multiple data and methods during 1957-2010. (2) Total water storage change driven by climate factors and its effects on discharge were explored. (3) The influences of climate change on glacier mass balance, glacier discharge and total discharge were discussed. (4) The effects of permafrost on hydrological regime were examined. Finally, climate sensitivity tests were applied to investigate changes in discharge under different climatic scenarios. Such case-studies can help to understand climate change impacts on the hydrological cycle by providing regional examples which are relevant for water resource management.

2. Study Area

The study area includes the upper catchment of the Shule River Basin which is located in the northeast Tibetan Plateau (96.6 ° -99.0° E, 38.2° -40.0° N) (Fig. 2a). The Shule River Basin is one of three largest inland rivers of China, located at the western end of the Hexi Corridor in northwestern China. It flows from southeast to northwest and is approximately 670 km long (Chang et al., 2016). The upper basin study area includes all areas above the Changma hydrological station located in the north-west (Fig. 2a). The basin area is 1.14×10^4 km^2, and the areas of glacier and continuous permafrost are 549 km^2 and 9447 km^2 which account for 5% and 83%, respectively (Sheng, 2010). The elevation ranges from 2100 to 5637 ma.s.l. (Figure 2a). The study area contains the main area of water conservation and flow for whole Shule River Basin. The spatial distribution map of frozen soil (Fig. 2b) was developed using the classification rules of Cheng and Wang (1982) using mean annual ground temperature (MAGT) data (Sheng *et al.*, 2010): extreme stable permafrost (MAGT ＜−5℃),stable permafrost (−5℃≤MAGT＜−3℃), sub-stable permafrost (−3℃ ≤ MAGT ＜-1.5℃), transition permafrost (−1.5℃≤ MAGT ＜ −0.5℃), unstable permafrost (−0.5℃≤ MAGT ＜ 0.5℃), and seasonal frozen soil areas (MAGT ≥

0.5℃). Meteorological stations are sparsely distributed over mountain regions such as this and there is just one station around the study area which is used for analyses of climate change (Fig. 2a). The annual average air temperature was approximately -2.6 ℃ from 1957 to 2010. Annual precipitation was 293.2 mm, with 92% occurring from May to September.

3. Datasets and methods

3.1 Datasets

(1) Meteorological, hydrological and glacier data

There is one national meteorological station around the study area (Tuole station, 98.42° E, 38.3° N, elevation: 3367 m) for which monthly temperature and precipitation data from 1957 to 2010 were obtained from the National Climate Centre of China (http://ncc.cma.gov.cn). The dataset has gone through the quality control procedures by Climate Data Center. Discharge were measured at the Changma hydrological station by the Hydrological Bureau. Annual total discharge was available from 1957 to 2010, and the monthly discharge was available from 1970 to 2006. As hydrological station is located in the mountainous regions, the discharge was observed as natural runoff, which was not affected by artificial drainage or irrigation. The data were assessed by plotting the time series and inspecting the possible errors and uncertainties (Kousari et al., *2013*). The Chinese Glacier Inventory project provided data on the spatial distribution of glaciers for study over two periods (1980s and 2000s) (http://westdc.westgis.ac.cn/). The four seasons are defined as spring (March to May), summer (June to August), autumn (September to November) and winter (December to February).

(2) GRACE data

The total water storage change is a key component in the hydrological cycle. The Gravity Recovery and Climate Experiment (GRACE) satellite provideds data that can be used for analyzing total water storage change (Rodell *et al*., 2004; Syed *et al*., 2008; Yang *et al*., 2013; Strassberg *et al*., 2014; Long *et al*., 2015; Deng and Chen, 2016). We obtained the GRACE data from the University of Texas Centre for Space Research (CSR), freely downloaded from the GRACE Tellus website (http://grace.csr.nasa.gov/data/get-data/). We used monthly time series of total water storage change from

2003 to 2014, presented spatially in 1° ×1° grid cells.

(3) Soil water content and snow water equivalent data

Soil moisture content and snow water equivalent come from the Global Land Data Assimilation Systems (GLDAS) Noah land surface model (http:// disc.sci.gsfc.nasa.gov/services/grads-gds/gldas) which includes four-layer soil water content with an assumed soil depth of 2 meters. It includes soil moisture and snow water equivalent. GLDAS data used here does not include changes of groundwater and separate surface water components. The GLDAS data also has a spatial resolution of 1° ×1° , consistent with GRACE data. We used the monthly time series of GLDAS from 2003 to 2014.

3.2 Methods

(1) Method of total water storage change data retrieval

This study uses GRACE Level-2 RL05 data. Current surface mass change data are based on RL05 spherical harmonics with order 60. Atmospheric pressure/mass changes have been removed and the C_{20} coefficients are replaced with the solutions from Satellite Laser Ranging (Cheng *et al*., 2011). Glacial isostatic adjustment (GIA) correction has been applied (Geruo *et al*., 2013). Correlated noises (N-S stripes) were removed from coefficients which used a fifth-order polynomial, it was fitted as a function for each odd or even set for a given order (Swenson and Wahr, 2006). Finally, the Gaussian averaging filter with a smoothing radius of 300 km is applied to calculate the total water storage change. These processed spherical harmonic coefficients were finally transformed into 1 degree resolution grids data.

Due to the sampling procedures and post-processing of GRACE observations, surface mass variations at small spatial scales tend to be attenuated. Therefore, the GRACE data should multiple the land data by the provided scaling grid. The scaling grid is a set of scaling coefficients, one for each 1 degree bin of the land grids, and are intended to restore much of the energy removed by the destriping, gaussian, and degree 60 filters to the land grids (Landerer and Swenson, 2012).

(2) Data masking for the study area

The spatial resolution of GRACE and GLDAS data are 1° ×1° in regular grid shape. However, the study area does not match with these grids. The area of intersection of each GRACE/ GLDAS grid cell with the watershed is estimated. The weight and estimation of GRACE/GLDAS are calculated by:

$$W_i = \frac{a_i}{g_i}$$
$$V_N = \frac{\sum_{i=1}^{n} V_i * W_i}{A} \quad (1)$$

where: W_i is the weight of grid cell i; a_i is the area of the watershed in the grid cell i with the GRACE/GLDAS data grid; g_i is area of 1° ×1° GRACE/GLDAS grid cell; V_N is the value of data of month N for the entire watershed; v_i is the value of the data of grid cell I; A is the total area of the watershed; and n is the number of the GRACE/GLDAS grid cells at least partially falling within the watershed.

(3) Estimation of evaporation

Since actual evaporation is difficult to acquire on the Tibetan Plateau, calculation of reference evapotranspiration is used to instead. The Penman-Monteith method is recommended as the standard method to estimate the ET, the physically based Penman-Monteith method is presently considered as the state-of-the art in estimation of evapotranspiration (Allen, 1998; Smith, 2000; Qiao and Zhu, 2017). Meteorological data at Tuole station was used. The equations can be expressed as (Yao *et al.*, 2008):

$$ET = \frac{0.408\Delta(Rn - G_{sfc}) + \gamma \frac{900}{T+273} u_2 (e_s - e_a)}{\Delta + \gamma(1 + 0.34u_2)} \quad (2)$$

$$e^0(T) = 0.618\, exp(\frac{17.27T}{T+237.3}) \quad (3)$$

$$e_s = \frac{e^0(T_{max}) + e^0(T_{min})}{2} \quad (4)$$

$$e_a = \frac{e^0(T_{max})\frac{RH_{min}}{100} + e^0(T_{min})\frac{RH_{max}}{100}}{2} \quad (5)$$

$$\Delta = \frac{4098\left[0.6108\exp(\frac{17.27T}{T+237.3})\right]}{(T+237.3)^2} \quad (6)$$

$$\gamma = 0.665\times10^{-3}P \quad (7)$$

where ET is the reference evapotranspiration (mm·d^{-1}), R_n is the net radiation (MJ·m^{-2}·d^{-1}), G_{sfc} is the soil heat flux at the ground surface (MJ·m^{-2}·d^{-1}), e_s is the saturation vapour pressure of the air temperature (KPa), e_a is the actual vapour pressure (KPa), γ represents a psychometric constant (KPa·℃$^{-1}$), T and u are the mean air temperature and wind velocity at a height of 2 m (m·s^{-1}), respectively. Δ is the slope of the saturation vapour-pressure curve of the air temperature (KPa·℃$^{-1}$), RH is the relative humidity, and P is the air pressure (KPa).

(4) Estimation of total water storage change and groundwater variations using the water balance equation

Water budget estimates of total water storage change can be calculated by water balance:

$$\Delta W = P - E - R \quad (8)$$

where ΔW is the total water storage change in the watershed (Woo *et al*., 1994; Li *et al*., 2010), P is the precipitation in watershed which can be estimated by calculating the precipitation gradients from nearby National Meteorological Stations in combination with their altitude, E is evaporation calculated by equations (2)-(7), and R is the runoff of watershed (measured as discharge).

GRACE-observed data represents the total change of terrestrial water storage, which include contributions from water storage changes in surface snow, subsurface soil, and groundwater (Chen *et al*., 2014a, b; Xiao *et al*., 2015). Therefore, when surface water storage change (in soil and snow) is known, the groundwater can be obtained after subtracting the GLDAS surface total water storage from the total water storage change derived by GRACE (Rodell *et al*., 2009; Jin and Feng 2013). Previous studies found a good agreement between GRACE estimated and in-situ observed groundwater variations (Feng *et al*., 2013; Cheng *et al*., 2014; Xiao *et al*., 2015; Long *et al*., 2016). The equation can be expressed as:

$$\Delta W = \Delta GW + \Delta SM + \Delta SWE \quad (9)$$

Where ΔW is the total change of total water storage change which can be retrieved by GRACE data, ΔGW is groundwater change, ΔSM and ΔSWE are the changes of soil moisture and snow water equivalent, which can be simulated from land surface hydrological models, herein, GLDAS.

(5) Calculation of glacial discharge in long term

Glacial discharge is defined as the discharge solely from glacier-covered areas (Li *et al.*, 2010). The components of runoff at hydrological station (Fig.2a) can be described as followed equation:

$$R_a = R - R_b \quad (10)$$

where R_a is glacial discharge, R is total discharge measured at the station and R_b is the non-glacial discharge in the study area. R_b can be calculated by followed expression:

$$R_b = P*(A_w - A_g)*\alpha \quad (11)$$

where P is precipitation in the catchment area (mm), A_w and A_g are the areas of the total watershed and of the glacier (m^2), respectively. α is the discharge ratio which represents the ability of runoff production, it is calculated by runoff and precipitation. We set several small sub-watersheds in different underlying in our study area (Fig. 3), and the runoff and precipitation were observed in these sub-watersheds in field work by rain gauge and HOBO water level gauge. The average α was calculated by these data. The observed average value of α in the study area is 0.21. Previous studies indicated that α was 0.18 in mountain regions of the northeast Tibetan Plateau (Zhu, 2008; Chen *et al*., 2014c). α in the study area is higher than in other watersheds which also include same underlying. The main reason is that precipitation is lower in our study area, and this tends to create a higher discharge ratio.

(6) Glacier mass balance calculated on the watershed scale

Since monitoring glacier mass balance over the long term can be difficult, especially over remote mountains, field observations are often combined with modelling to determine the glacier mass balance. Previous works have indicated that precipitation and runoff have negative exponential relationships with the relative areas occupied by glaciers on the watershed scale in the western mountains of China (Shen *et*

al., 1997). Precipitation, runoff and runoff coefficients exhibit maximum values in watersheds with high glacier surface area. Based on the statistical mechanics and maximum entropy principle (SMMEP) model, formulas for calculating glacier mass balance in watersheds with hydrological and meteorological observations are as follows:

$$R_g = R - (R - R_0)\ln(F_g/F) \quad (12)$$

$$P_g = P - (P - P_0)\ln(F_g/F) \quad (13)$$

$$\alpha_g = \alpha - (\alpha - \alpha_0)\ln(F_g/F) \quad (14)$$

where R_g, P_g and α_g are the average depth of the runoff, precipitation and runoff coefficient on the glacier, respectively; R, P and α are the average depth of the runoff, precipitation and runoff coefficient in the watershed as a whole, respectively; R_0, P_0 and α_0 are the minimum values of the runoff, precipitation and runoff coefficients in the watershed, respectively; F_g is the area covered by glaciers in the watershed, and F is the area of the watershed (Shen *et al.*, 2001).

According to the principle of water balance, the ratio between the glacier runoff and watershed runoff observed at hydrological station (K_{GR}) is therefore:

$$K_{GR} = (F_g/F)\{1 + [\alpha_B(FP - F_gP_g) - (FR - F_gR_g)]/(R_gF_g)\} \quad (15)$$

where α_B is the runoff coefficient for a bare region, which can be calculated as follows:

$$\alpha_B = (\alpha F - \alpha_g F_g)/(F - F_g) \quad (16)$$

The ratio of precipitation at the hydrological station to precipitation on the glacier (K_{GP}) can be calculated as follows:

$$K_{GP} = P_h/P_g \quad (17)$$

where P_h is the average annual precipitation at the hydrological station. In our study, observations of precipitation in the watersheds or at the hydrological stations are not available. However, the study area is located in Qilian Mountains where precipitation increases with altitude (Liu *et al.*, 2011). Therefore

precipitation in watershed can be estimated by calculating the precipitation gradients from nearby National Meteorological Stations in combination with their altitude. The precipitation lapse rate is 4.6 mm/100 m at elevations representative of our study area (Liu *et al.*, 2011).

Based on the glacier mass balance principle, glacier mass balance can be calculated as follows:

$$B_i = C_i - A_i \quad (18)$$

$$C_i = P_{hi}/K_{GP} \quad (19)$$

$$A_i = R_i/K_{GR} \quad (20)$$

where C_i (mm) is the annual glacier accumulation in the watershed, A_i (mm) is the annual glacier ablation, B_i (mm) is the annual glacier mass balance in the watershed, P_{hi} (mm) is the precipitation at the hydrological station, and *i* represents the year during the study period.

(7) Analyse the effects of permafrost on hydrological regime

Given the difficulty in surveying permafrost degradation across a basin, it is difficult to investigate directly the influence of permafrost degradation on the streamflow. The ratio between the maximum runoff and minimum runoff directly links stream flow regime with basin permafrost coverage (Ye *et al*., 2009). In this study, we used the ratio of [Q_{max}/Q_{min}] and the minimum flow to indirectly reflect changes in basin permafrost. The ratio of monthly flows between consecutive months, or monthly recession coefficient (RC), was used to quantify measure of recession processes.

(8) Mann-Kendall monotonic trend test

Mann-Kendall monotonic test was applied to detect trends in hypothesis testing of hydro-meteorological time series which is without specifying whether the trend is linear or nonlinear (Kendall and Stuart, 1973). In the Mann-Kendall monotonic trend test, the null hypothesis (H_0) assumes that there is no significant increased or decreased trend in the time series, while the time series has a significant variation trend based on the alternative hypothesis (Li *et al.*, 2012; Ling *et al.*, 2013). The test statistic (*S*) is described by the following equation:

$$S = \sum_{i=1}^{n-1} \sum_{j=i+1}^{n} sgn(x_j - x_i) \quad (21)$$

x_i is a time-series from i=1, 2, 3...n -1, and x_j is another time-series from j=i+1,., n, x_j is greater than x_i, n is the data set record length. Each point x_i is used as a reference point of x_j, the results are recorded as sgn (θ):

$$sgn(\theta) = \begin{cases} 1, \theta > 0 \\ 0, \theta = 0 \\ -1, \theta < 0 \end{cases} \quad (22)$$

If the data set is identically and independently distributed, then the mean of S is zero and the variance of S is as follow:

$$Var[S] = \left[n(n-1)(2n+5) - \sum_t t(t-1)(2t+5) \right] \Big/ 18 \quad (23)$$

Where n is the length of the data set, t is the extent of any given tie, and represents the sum over all ties. Then, the test statistic is given as Z_c. For a long time-series, statistical value S can be transformed into Z_c, the calculation equation is as follows:

$$Z_c = \begin{cases} \dfrac{S-1}{\sqrt{var(S)}}, & S > 0 \\ 0, S = 0 \\ \dfrac{S+1}{\sqrt{var(S)}}, S < 0 \end{cases} \quad (24)$$

When Z_c is $-1.96 \le Z_c \le 1.96$, the null hypothesis (H_0) is accepted, which indicates that there is no obvious trend in the samples. The trend is significant at the 95 % confidence level if $|Z|>1.96$ and at the 99 % confidence level if $|Z_c|>2.58$. A positive Z_c indicates that the sequence has an increased trend, while a negative Z_c reflects a declining trend (Kendall and Stuart, 1973). Besides identifying whether a trend exists, the Kendall inclination is usually used to detect the monotonic trend. The magnitude of trend can be defined as follows:

$$\beta = Median\left(\frac{x_i - x_j}{i - j} \right), \forall j < i \quad (25)$$

where $1 < j < i < n$, positive β indicates an increased trend, and negative β indicates a decreased trend.

4. Results and analysis

4.1 Temperature and precipitation changes

Fig. 4 shows the variations of mean annual, spring, summer, autumn and winter temperature Tuole station, respectively. The Mann-Kendall monotonic trend test statistics, which reached a significance level of 0.01 ($|Zc| > 2.58$), showed that the temperatures increased significantly with fluctuations from 1957 to 2010 (Tab. 1). A rapid increase in the mean annual temperature occurred around in 1985, which was consistent with the climate jump on the Tibetan Plateau during the mid-1980s (Ding and Zhang, 2008), the other rapid increase turned up in 1995. The Mann-Kendall slopes (β) indicated monotonically increasing trends. The average temperature increase rate was 0.34℃/10 years in the Tuole station (Tab. 1). Annual temperature has increased by around 1.8℃ from 1957 to 2010. The highest temperature occurred in 1998, previous study also indicated that 1998 was the warmest year during the 1990s in China (Chen *et al*., 2004). The temperature in spring, summer, autumn and winter increased at a rate of 0.20, 0.27, 0.39 and 0.62 ◦ C/10 years, respectively, which all reached a significance level of 0.01 ($|Zc| > 2.58$). The most significant warming occurred in winter, the lowest rate is spring. The results suggest that annual and each season's warming were remarkable in the study area during past several decades.

Fig. 5 shows the variations of mean annual, spring, summer, autumn and winter precipitation in Tuole station, respectively. The annual precipitation increased significantly with fluctuations from 1957 to 2010 (Tab. 2). The precipitation increase rate is 13.5 mm/10 years (Tab. 2). Annual precipitation has increased by around 71.6 mm from 1957 to 2010. The wettest year is 1998 which is consistent with the warmest year. Comparing to the 1950s, the annual precipitation in the 2000s has increased by 23.1% (62.18 mm). The variations of precipitation in spring, autumn and winter were complicated which showed different trend. The test statistic of Z_c for the spring precipitation was -0.06 (Tab. 2), indicating that precipitation experienced a slight downtrend with a rate of -0.06 mm/10 years. The increasing rates of precipitation in summer, autumn and winter were 11.2, 3.9 and 0.1 mm/10 years, respectively. Except in winter, the

increasing rates in other seasons exceeded the significance level of 0.01 (|Zc| > 2.58). The mean annual precipitation in spring, summer, autumn and winter are 47.0 mm, 204.1 mm, 38.6 mm and 3.6 mm in the Tuole station.

4.2 Discharge variation and contribution of glacier discharge to river flow

The Mann-Kendall monotonic trend of discharge is shown in Fig. 6a. It can be seen that during 1957-2010 the discharge is in significant increasing trend at a test level of 0.01 in the upstream of Shule River Basin (|Zc| > 2.58)(Tab. 3). The increasing rate of discharge was 7.9 $\times 10^6$ m^3/year. A rapid increase in the annual discharge occurred around in 1995 when the temperature also has a significant increase. The discharge in spring, summer, autumn and winter increased at a rate of 0.74×10^6 m^3/year, 5.2×10^6 m^3/year, 1.3×10^6 m^3/year and 0.7 $\times 10^6$ m^3/year from 1970 to 2006, respectively, which all reached a significance level of 0.01 (|Zc| > 2.58). The discharge in winter and autumn is quite low, increase of discharge primary occurred in summer.

The glacial discharge was calculated by equation (10) and (11). The glacial discharge has increased during 1957-2010 in the study area (Fig. 6a). Total glacier discharge was approximately 187.99×10^8 m^3 during 1957-2010. Total discharge and glacier discharge have varied significantly during study period, generally exhibiting an increasing trend. The impact of glacier discharge on river flow has increased, the cumulative annual river flow and glacier discharge anomalies indicated that 1996 is a key year, when a strong decreasing trend shifted to a strong increasing phase (Fig. 6c). The decadal statistics showed that glacier discharge continued to increase (Tab. 4). The mean glacier discharge was 2.83×10^8 m^3 for 1950s and 3.23×10^8 m^3 for 1990s. Glacier discharge reached a maximum in the 2000s, with a mean annual glacier runoff of 2.83×10^8 m^3. The Glacier discharge during the 2000s is 44.7% of the total discharge, whereas it accounted for 34.4% of the total river flow from 1957 to 2010. The minimum percentage of glacier discharge occurred in 1980s, however, the minimum glacier discharge occurred in 1960s (Tab. 4).

4.3 Glacier mass balance variation

In the glacierized watershed, the glacier mass balance reflects the response of glacier movement to climate change and also controls changes in stream flow and glacier variations during periods of ablation (Braithwaite and Zhang, 2000; Barnett *et al.*, 2005; Stahl *et al*., 2008). The glacier mass balance was calculated by equation (12)-(20). The method has been applied in Glacier No. 1 of Tianshan Mountains and Kang Xi Wa River basin of east Pamirs, the model performed well in results which agree well with observations (Shen et al., 1997). The result simulated by SMMEP model were compared with Qiyi Glacier in this region. The cumulative glacier mass balance are close between Qiyi Glacier and the glaciers of study area, glacier mass balance trend was consistent with Qiyi Glacier which showed a modest increasing trend from 1957 to 1994 and rapidly decreasing trend since then (Yao *et al*., 2012). Fig. 7a shows that annual glacier mass balance varied between 197.8 and -535.5 mm during 1957-2010. The cumulative mass balance was positive before 2000, and it has been decreasing rapidly during 2000s. The most and significant negative mass balance almost all appeared after 1996. Cumulative mass balance reached -3370 mm over the study period. The mean annual glacier mass balance was positive in 1980s with 14.9 mm, while in the 2000s, the most negative value occurred, the mean annual glacier mass balance reached -226.2 mm (Fig. 6a). The impact of glacier mass balance loss on river flow was more evidently after 2000.

4.4 Evapotranspiration (ET) variation

Fig. 8 shows the annual and seasonal ET trends during 1957-2010 for Tuole station calculated by equation (2)-(7). The Mann-Kendall monotonic trend test statistics, which reached a significance level of 0.01 ($|Zc| = 4.92 > 2.58$), showed that the annual ET increased significantly with fluctuations (Tab. 5). The ET increasing rate was 1.34 mm/year. Annual mean ET was 297.6 mm from 1957 to 2010. An increasing trend was found from the 1950s to early 1985, followed by a decrease until 1995, and then a evident increase until 2010. Comparing to the 1950s, the annual ET in the 2000s has increased by 11.8% (35.0 mm). According to Mann-Kendall monotonic trend test statistics, the ET showed a increasing trend in four seasons. The increasing magnitudes of ET trend were 0.083 mm/year, 0.97 mm/year, 0.27 mm/year and 0.013 mm/year for spring, summer, autumn, and winter, respectively (Tab. 5). However, increasing trends just in summer and autumn were significant with a significance level of 0.01, which reflected the seasonal

differences in ET trend. The values of ET were 67.7 mm, 171.4 and 55.3 mm in spring, summer, autumn, respectively. It was quite low in winter, the annual mean ET was 5.7 mm.

4.5 Estimate total water storage change and groundwater variations

Fig. 9a shows the total water storage change estimated based on the water balance in the upstream of Shule River Basin (equation (8)). The total water storage change calculated by water balance showed an obviously decreasing trend with a rate of 0.788 mm/year. Although the changes of precipitation and ET were also evident increase, their amplitudes of variation were far less than increase of discharge. The result indicated that continuously increasing discharge amounts lead to a reduction of water storage. Fig. 9b illustrated the time series of total water storage change and soil water content which derived by GRACE and GLDAS, both of them showed decreasing trend since 2003. The soil water content change from GLDAS showed a larger amplitude than the GRACE-derived total water storage change . The total water storage change and soil water content agree relatively well in time series except for 2004. The GRACE-derived total water storage change showed a decreasing trend from 2003 to 2014 with a decline of 5.92 mm/year. The maximum anomaly of GRACE-derived total water storage change was 66.23 mm and occurred in 2004, while the minimum anomaly of about -90.93 mm occurred in 2014. The maximum anomaly of soil water content change was 68.57 mm and occurred in 2008, while the minimum was about -246.51 mm occurred in 2014.

The changes in groundwater were estimated by the difference between GRACE-derived total water storage change and simulated soil water content change (equation (9)). The groundwater showed an increasing trend during 2003-2014 in the upstream of Shule River Basin (Fig. 9c). Fig. 9c also showed a distinct break in the behavior of groundwater variations. The groundwater showed a dramatic depletion from 2004 to 2007 which means more water flow out the study area to change into discharge, and then an evident increase until 2014 which means more water change into groundwater. The permafrost has underwent degradation in the study area as climate warming (Yi *et al*., 2011). Previous study indicated groundwater increased with decreasing permafrost coverage. The maximum value of groundwater is 155.58 mm and occurred in 2014, while the minimum was about -90.49 mm occurred in 2006. The mean depth of groundwater is 23.82 mm in the upstream of Shule River Basin during 2004-2014.

Fig. 9d shows monthly variability of GRACE-derived total water storage change, GLDAS-soil water content change and groundwater in the study area from 2003 to 2014. The results showed that the all variables exhibited higher values in summer and lower values in winter. The value of GRACE-derived total water storage change was positive from July to November, and it showed negative value in other months. The soil water content change from GLDAS showed positive value from September, and in other months the value was negative. The groundwater has longest positive value from May to November, and the maximum value occurred in July (13.73 mm). Both maximum and minimum value of the soil water content change lagged total water storage change one month. The positive peaks of GRACE-derived total water storage change, GLDAS-soil water content change and groundwater in summer due to abundant recharge from meltwater from glaciers and precipitation.

5. Discussions

5.1 The influences of climate change on glacier mass balance, glacier discharge and total discharge

Temperature and precipitation changes affected differently on glacier mass balance. Precipitation increased enhance accumulation, and temperature warming enhanced ablation (Ye *et al*, 2005). The negative glacier mass balance, caused by higher ablation than the accumulation, was associated with precipitation increase and temperature warming over the study area. The fluctuation of total runoff depth was not consistent with glacier mass balance before 1990s (Fig. 7). The glacier mass balance in the study area was determined by both precipitation and temperature before 1986 (R^2=0.2111, $p<0.05$), whereas after 1986 it is mainly controlled by the temperature (R^2=0.4914, $p<0.05$), even under a high-precipitation regime (Fig. 10). The results implied that the effect of warming overcame the influence of precipitation increase in the upstream of Shule River Basin.

The variation of glacier mass balance reflects the budget of the glacier system. Higher ablation than accumulation induced the negative mass balance. Regression analysis showed that glacier discharge and total discharge were obviously negatively correlated with glacier mass balance (Fig. 11). The correlation of glacier discharge and total discharge with glacier mass balance gave an R coefficient of −0.9389 and 0.5813 ($p<0.01$), respectively. This relationships between glacier discharge, total discharge and glacier

mass balance were reasonable, as a more negative mass balance led to a larger amount of glacier melt which led larger total discharge. The variation of glacier discharge was controlled mainly by the fluctuation of glacier mass balance. Glacier discharge significantly increased as a result of temperature increases.

The climate regime shifted from cold-dry to warm-wet, occurring around 1995. Tab. 6 listed the average precipitation, air temperature, glacier mass balance, glacier discharge and total discharge during 1957-1994 and 1995-2010 in the study area. Glacier discharge increased by approximately 23.6 mm (2.60×10^8 m^3), about 95.2%, whereas precipitation increased by 27.1 mm (9.5%), and there was a 1.15 ℃ increase in temperature, and -185.9 mm decrease in glacier mass balance. This indicated that about 10% of glacier discharge came from increases in precipitation, and another 85.2% was contributed by the loss of glacier mass. The discharge increased by 3.32×10^8 m^3 (39.6%), of which approximately 9.5% was contributed by increase in precipitation, and the other 30.1% came from glacier discharge. It meant that the increased glacier discharge accounted for 72.4% of the increased river flow. The 1.15 ℃ increase of temperature caused a -185.9 mm annual glacier mass loss, which was partly compensated by a 27.1 mm increase in annual precipitation. This was equal to a change in glacier mass balance of -161.7 mm/℃ without increasing precipitation. By analyzing the river flow and glacier mass balance, we found that a 100 mm change in mass balance could cause a fluctuation in river discharge of 1.79×10^8 m^3. The total cumulative glacier mass balance from 1957 to 2010 was -3370.6 mm, equal to a 60.33×10^8 m^3 contribution to river discharge, which was about 6.3 times the annual discharge at gauging station. The changes of hydrological regime in the region not only was linked to the climate changes, but also impacted by glacier conditions, which further emphasized that glacial meltwater is very importance as a local water resource.

5.2 Effects of permafrost on hydrological regime

The permafrost affected the spatial-temporal hydraulic connection between the groundwater and surface water, and it played a decisive role in the formation of groundwater, the transport processes, and the pattern of distribution of groundwater and its pathways (Lemieux et al., 2008; Woo et al., 2008). Fig. 12 shows the monthly maximum, minimum depth of runoff and the ratio of [R_{max}/R_{min}] in the study area from1970 to 2006. The monthly maximum runoff fluctuated between 12.1 and 42.8 mm, with an average

of 24.0 mm, which had an upward trend during 1970-2006. Monthly minimum runoff ranged from 1.2 to 3.2 mm, with a mean of 2.1 mm, and there was a positive trend during the study period. The R_{max}/R_{min} ratio varied from 6.8 to 25.5, with a mean of 11.7. It had a slight decreasing trend which indicated the trend in monthly minimum stream flow was greater than that in maximum stream flow (Fig. 12b). Previous study suggested that minimum flow was most sensitive to the subsurface water contribution to river discharge (Smith *et al*., 2007). Therefore, the variation of R_{max}/R_{min} ratio in the result indicated that the basin storage and the mechanism of discharge generation have changed.

It is difficult to survey permafrost change over large regions. As no other liquid water supply to the rivers discharge in cold regions during cold periods, disappearance of permafrost or thickening of the active layer increased groundwater storage capacity, which enlarged groundwater regulation and slows recession (Niu *et al*., 2016). Groundwater storage capability can be described as the recession coefficient (RC) which is the ratio of monthly discharge between consecutive months (Ye *et al*., 2009). The mean monthly RC in the study area ranged from 0.57 in early autumn (October/September) to 1.01 in later winter (January/December), indicating fast recession in early autumn and slow in late winter. The time series of RC showed increasing trend in October /September and January/December, whereas a decreasing trend in November/October and December/November (Fig. 13). Permafrost change has induced the changes of discharge recession which is generally a process of storage and release. Winter discharge increased as covered by permafrost. On the other hand, thin permafrost had greater impacts on ice formation during the freezing season and greater impacts on the baseflows during the thawing season, and the mutual influences of groundwater and surface waters were significant in the permafrost regions (Zhang et al., 2008; Gao et al., 2016; Qin et al., 2017). The ratio of groundwater discharge to total discharge and the direct surface discharge coefficient simultaneously increased during summer (Wang et al., 2012, 2017). The runoff increased more obviously in summer (Tab. 3). Ground warming led to higher permeability and wetter aquifers in the permafrost. The increase and thickening of the active layer could lead to the greater infiltration of surface water into the groundwater, and then resulting in increased total runoff.

5.3 Total water storage change driven by climate factors and its effects on discharge

Climate change is an important factor affecting total water storage change variations. There was a significant negative correlation between annual total water storage change and annual temperature (Tab. 7). The annual temperature increased lead to total water storage change decreased. In summer and winter, the correlation also showed negatively, it was more obvious in winter, whereas the correlation was positive in spring which meas the higher temperature induced higher total water storage change. The soil water content change simulated by GLDAS had a positive correlation with temperature in autumn and a negative correlation in winter, but no significant correlation was observed in annual temperature and other seasons. The total water storage change had significant positive correlations with precipitation in winter, and negative correlation in spring (Tab. 8). The soil water content change showed a negative correlation with precipitation in spring, and the correlation was positive in summer, autumn and winter. The annual and seasonal total water storage change were mainly controlled by temperature variation, whereas the soil water content change was controlled by precipitation variation. At the annual scale, anomalies in the three hydrological variables show different relationships with total runoff anomalies in the upstream of Shule River Basin (Fig. 14), both total water storage change and groundwater had a strong negative correlation with total runoff anomalies with R^2 of 0.7891 and 0.4077, respectively, but no significant correlation was observed between SM (Soil Moisture) and total runoff anomalies. Specifically, changes in annual total water storage change and groundwater change explain 79% and 41% of the changes in annual runoff, respectively, suggesting a strong hydrological control on water budget in surface discharge in the upstream of Shule River Basin.

5.4 Sensitivities of discharge under different climate scenarios

As the discharge in cryospheric watershed was influenced by precipitation and temperature. Regression analysis and statistical tests proved that temperature in ablation season (May-September) and annual precipitation were the governing factor affecting the discharge. Both precipitation and temperature showed well linear relationship with discharge (Tab. 9). Firstly, liner relation between discharge and precipitation and temperature was established (equation (3) in Tab. 9). However, in consideration of the nonlinear relations between hydrology and water resources system and climate change, a form of continual

product of power function was used to describe the relations among runoff depth, precipitation and ablation season temperature in the upstream of Shule River Basin. Nonlinear model had better relationship than linear relationships in the region. Figure 15 shows the comparison of observation and simulation by equation (4) in Tab. 9, which illustrate the satisfactory accuracy of this equation.

Climate sensitivity tests are performed to investigate changes in discharge as a result of ablation season temperature and annual precipitation changes using a delta-change method in the study area. Previous study suggested that annual precipitation annual temperature in whole Tibetan Plateau were generally projected to increase by 5.0-20.0% and 1.2-4.0℃ in the long term under scenarios RCP2.6, RCP4.5, and RCP8.5 (Su et al., 2016). Therefore, considering the regional characteristics of climatic change, the climate change scenarios are that the precipitation change scenes are 0%, ±5%, ±10%, ± 20%, simultaneously, the temperature increases by 0 ℃, 0.5 ℃, 1℃ and 2℃, which are together with possible combinations (Tab. 10). Tab. 9 shows the the response of runoff to different climate variations by using equation (4) in Tab. 8. The runoff will increase along with the precipitation and temperature increase, and that the increased extents gradually increase along with increased extent of precipitation and temperature. The decreased in precipitation will lead to a reduction in runoff under same temperature scenarios. However, even in the case of reduced precipitation, an increase in temperature will lead to increased runoff except for precipitation reduction of more than 20% under temperature increasing by 0.5 ℃. The impacts of temperature are more evident than precipitation. The results suggest that the impact of warming will overcome the effect of precipitation increase on runoff changes in the upstream of Shule River Basin.

5.5 Uncertainties in estimation of glacier mass balance

The glacier area is one parameter in the calculation of glacier mass balance which is influenced by climate change. The glacier area of the northeast Tibetan Plateau changed in past several decades (Liu *et al*., 2015). The model applied in study used two periods of glacier area. As the changes of glacier area are dynamic processed in different periods which made some uncertainties in this study and other studies (Hagg *et al*., 2007; Li *et al*., 2010; Zhang *et al*., 2012). Glacier changes mainly depend on the precipitation and temperature regime (Hagg et al., 2007). Glacier melt dominates partly river flow in glacierized

watersheds. Such melt characteristics of glaciers was severely affected by changes in discharge and precipitation. Glacier shrinkage led to a mass loss of glaciers, which stored precipitation and released it to feed stream flow to increase discharge. Precipitation change affected glacier melt and the area of ablation zone of glaciers (Caidong and Sorteberg, 2010). Simultaneous constraints to the glacier mass balance simulation reached agreement with measured glacier mass balance (Qiyi Glacier). The results of glacier mass balance help to reveal the impacts of climate change on glacier and hydrological processes in the watershed of the northeast Tibetan Plateau.

6. Conclusions

In this study, the influence of climate change on cryospheric water budget was analyzed in the upstream of Shule River Basin which is located in northeast Tibetan Plateau. The following conclusions could be drawn from results.

(1) The study area experienced an overall rapid warming and wetting during 1957-2010. The temperature increase rate was 0.34℃/10 years. Annual temperature has increased by around 1.8℃ from 1957 to 2010. Warming is the most significant in winter with an average rate of 0.62℃/10 years and the smallest in spring (0.20℃/10 years). The annual precipitation increased with a rate of 13.5 mm/10 years from 1957 to 2010. Annual precipitation has increased by around 71.55 mm. The maximum increase of the precipitation occurred in summer with a rate of 11. 2 mm/10 years. The climate regime shifted from cold-dry to warm-wet, occurring around 1995.

(2) Annual total discharge and glacier discharge exhibited increasing trends. A noticeable increase occurred after 1995. The increasing temperature enhanced ablation of glacier. The glacier mass balance has displayed a decreasing trend. A more negative glacier mass balance led to a larger amount of glacier melt which led larger total discharge. The effect of warming overcame the influence of precipitation increase after 1986. Glacier discharge accounted for 34.4% of the total river flow from 1957 to 2010 while it accounted for 44.7% after 2000s. Permafrost change also induced the changes of discharge recession which is generally a process of storage and release.

(3) The ET showed increasing trend with rate of 1.34 mm/year. Based on water balance, the total

water storage change showed an obviously decreasing trend with a rate of 0.788 mm/year from 1957 to 2010. The total water storage change and soil water content change which derived by GRACE and GLDAS also showed decreasing trend since 2003. The groundwater increased dramatically after 2006, as permafrost degraded, surface water can infiltrate groundwater and eventually leak water deep into the ground. Both total water storage change and groundwater change had a negative correlation with total runoff which suggest a strong hydrological control on water cycle in surface discharge. As ET is almost equivalent to precipitation, the sensitivities of runoff to temperature change is larger than that to precipitation change. The impact of warming will overcome the effect of precipitation increase on runoff changes in the study area. The climate change has lead the changes of cryosphere which induced the changes of water budget in different fractions.

Acknowledgement

We thank NASA for providing the GRACE and GLDAS data. The authors would like to thank the editors and the anonymous reviewers for their crucial comments, which improved the quality of this paper. This study was supported by the Strategic Priority Research Program of the Chinese Academy of Sciences (XDA19070302), the National Natural Science Foundation of China (41721091, 41501073), the CAS Pioneer Hundred Talents Program (Xiaoming Wang), the project of State Key Laboratory of Cryospheric Science (SKLCS-ZZ-2018), and Natural Science Foundation of Gansu Province (1606RJZA104), Youth Innovation Promotion Association CAS (Xu Min).

References

Allen RG, Pereira LA, Raes D, Smith M. 1998. Crop evapotranspiration: guidelines for computing crop water requirements. FAO Irrigation and Drainage Paper 56. FAO, Rome, Italy, p. 293.

Braithwaite RJ, Zhang Y. 2000. Sensitivity of mass balance of five Swiss glaciers to temperature changes assessed by tuning a degree-day model. *Journal of Glaciology* 46: 7-14.

Bolch T, Kulkarni A, Kääb A, Huggel C, Paul F, Cogley JG, Frey H, Kargel JS, Fujita K, Scheel M, Bajracharya S, Stoffel M. 2012. The state and fate of Himalayan glaciers. *Science* 336: 310-314.

Barnett TP, Adam JC, Lettenmaier DP. 2005. Potential impacts of a warming climate on water availability in snow-dominated regions. *Nature* 438: 303-309.

Cheng GD, Wang SL. 1982. On the zonation of high-altitude permafrost in China. *Journal of Glaciology and Geocryology* 4 (2): 1-17.

Chen L, Zhou X, Li W. 2004. Characteristics of the climate change and its formation mechanism in China in the last 80 years. *Acta Meteorologica Sinica* 62: 634-646.

Chen S, Liu Y, Thomas, A. 2006. Climatic change on the tibetan plateau: potential evapotranspiration trends from 1961-2000. *Climatic Change*, 76(3-4): 291-319.

Caidong, C., & Sorteberg, A. 2010. Modelled mass balance of xibu glacier, tibetan plateau: sensitivity to

climate change. *Journal of Glaciology* 56: 235-248.

Cheng MK, Ries JC, Tapley BD. 2011. Variations of the Earth’ sfigure axis from satellite laser ranging and GRACE. *Journal of Geophysical Research* 116: B01409.

Chen J, Li J, Zhang Z, Ni S. 2014a. Long-term groundwater variations in northwest India from satellite gravity measurements. *Global & Planetary Change* 116(1): 130-138.

Chen R, Yang Y, Han C, Liu J, Kang E, Song Y, Liu Z. 2014c. Field experimental research on hydrological function over several typical underlying surfaces in the cold regions of western China. *Advances in Earth Science* 29(4): 507-514.

Chang Y, Ding Y, Zhao, Q, Zhang S. 2016. Remote estimation of terrestrial evapotranspiration by landsat 5 TM and the sebal model in cold and high-altitude regions: a case study of the upper reach of the Shule river basin, china. *Hydrological Processes* 31(3): 514-524.

Chen J, Li J, Zhang Z, Ni S. 2014b. Long-term groundwater variations in northwest india from satellite gravity measurements. *Global & Planetary Change* 116(1): 130-138.

Cao X, Hu L, Wang J, Wang J. 2017. Regional Groundwater Flow Assessment in a Prospective High-Level Radioactive Waste Repository of China. *Water* 9: 551.

Ding Y, Zhang L. 2008. Intercomparison of the time for climate abrupt change between the Tibetan Plateau and other regions in China (Chinese with English abstract). *Chinese Journal of Atmospheric Science* 32: 794-805.

Duethmann D, Peters J, Blume T, Vorogushyn S, Güntner A. 2014. The value of satellite‐derived snow cover images for calibrating a hydrological model in snow‐dominated catchments in central asia. Water Resources Research, 50(3): 2002-2021.

Deng H, Chen Y. 2016. Influences of recent climate change and human activities on water storage variations in central asia. *Journal of Hydrology* 544: 46-57.

Famiglietti JS, Lo M, Ho SL, Bethune J, Anderson KJ, Syed TH, Swenson SC, de Linage CR, Rodell M. 2011. Satellites measure recent rates of groundwater depletion in california's central valley. *Geophysical*

Research Letters 38(3): 403-406.

Feng W, Zhong M, Lemoine JM, Biancale R, Hsu HT, Xia J. 2013. Evaluation of groundwater depletion in North China using the Gravity Recovery and Climate Experiment (GRACE) data and ground-based measurements. *Water Resources Research* 49: 2110–2118.

Gao H, He X, Ye B, Pu J. 2012. Modeling the runoff and glacier mass balance in a small watershed on the central tibetan plateau, china, from 1955 to 2008. *Hydrological Processes* 26(11): 1593-1603.

Gao T, Zhang T, Lin C, Kang S, Sillanpää M. 2016. Reduced winter runoff in a mountainous permafrost region in the northern Tibetan Plateau. *Cold Regions Science and Technology* 126: 36-43.

Gao H, Han T, Zhao Q, Liu L. 2016. Use of auxiliary data of topography, snow and ice to improve model performance in a glacier dominated catchment in Central Asia. *Hydrology Research* doi: Hydrology-D-16-00142.

Gao H, Ding Y, Zhao Q, Hrachowitz M, Savenije HHG. 2017. The importance of aspect for modelling the hydrological response in a glacier catchment in Central Asia, *Hydrological Processes* 31 (16): 2842-2859.

Geruo A, Wahr J, Zhong S. 2013. Computations of the viscoelastic response of a 3-d compressible earth to surface loading: an application to glacial isostatic adjustment in Antarctica and Canada. *Geophysical Journal International* 192(2): 557-572.

Hobbins MT, Ramírez JA, Brown TC. 2004. Trends in pan evaporation and actual evapotranspiration across the conterminous US: Paradoxical or complementary ? *Geophysical Research Letters* 31(13): 405-407.

Hagg W, Braun LN, Kuhn M, Nesgaard TI. 2007. Modelling of hydrological response to climate change in glacierized central asian catchments. *Journal of Hydrology* 332: 40-53.

Immerzeel WW, van Beek LP, Bierkens MF. 2010. Climate change will affect the Asian water towers. *Science* 328: 1382-1385.

Jin S, Feng G. 2013. Large-scale variations of global groundwater from satellite gravimetry and hydrological models, 2002-2012. *Global & Planetary Change* 106(3): 20-30.

Kendall MG, Stuart A. 1973. *The Advanced Theory by Statistics*. Griffin, London.

Kang S, Xu Y, You Q, Flügel W, Pepin N, Yao T. 2010. Review of climate and cryospheric change in the Tibetan Plateau. *Environmental Research Letters* 5: 015101.

Kousari MR, Zarch AA, Ahani H, Hakimelahi H. 2013. A survey of temporal and spatial reference crop evapotranspiration trends in Iran from 1960 to 2005. *Climate Change* 120: 277-298.

Kang S, Wang F, Morgenstern U, Zhang Y, Grigholm B, Kaspari SM, Schwikowski Ren J, Yao T, Qin D, Mayewski PA. 2015. Dramatic loss of glacier accumulation area on the Tibetan Plateau revealed by ice core tritium and mercury records. *The Cryosphere* 9(3): 1213-1222.

Lawrimore JH, Peterson TC. 2000. Pan evaporation trends in dry and humid regions of the United States. *Journal of Hydrometeorology* 1(6): 543-546.

Liu S, Ding Y, Li J, Shangguan D, Zhang Y. 2006. Glaciers in response to recent climate warming in western China. *Quaternary Science Reviews* 26: 762-771.

Li Z, Wang W, Zhang M, Wang F, Li H. 2010. Observed changes in streamflow at the headwaters of the Urumqi river, eastern Tianshan, Central Asia. *Hydrological Processes* 24(2): 217-224.

Liu XM, Zheng HX, ZhangMH, Liu CM. 2011. Identification of dominant climate factor for pan evaporation trend in the Tibetan Plateau. *Journal of Geographical Sciences* 21(4): 594-608.

Liu JF, Chen RS, Qin WW, Yang Y. 2011. Study on the vertical distribution of precipitation in mountainous regions using TRMM data. *Advances in Water Science* 22: 447-454. (in Chinese)

Landerer, F.W., Swenson, S.C. 2012. Accuracy of scaled GRACE terrestrial water storage estimates. *Water Resources Research* 48 (4): 4531.

Li BF, Chen YN, Chen ZS, Li WH. 2012. Trends in runoff versus climate change in typical rivers in the arid region of northwest China. *Quaternary International* 282: 87-95.

Ling HB, Xu HL, Fu JY. 2013. Temporal and spatial variation in regional climate and its impact on runoff in Xinjiang, China. *Water Resource Management* 27: 381-399.

Liu SY, Yao XJ, Guo WQ, Xu JL, Shangguan DH, Wei JF, Bao WJ, Wu LZ. 2015. The contemporary glaciers

in china based on the second chinese glacier inventory. *Acta Geographica Sinica* 70: 3-16.

Long D, Longuevergne L, Scanlon BR. 2015. Global analysis of approaches for deriving total water storage changes from GRACE satellites. *Water Resources Research* 51 (4): 2574-2594.

Long D, Chen X, Scanlon BR, Wada Y, Hong Y, Singh VP, Chen Y, Wang C, Han Z, Yang W. 2016. Have GRACE satellites overestimated groundwater depletion in the Northwest India Aquifer? *Scientific Report* 6: 24398.

Niu L, Ye B, Ding Y, Li J, Zhang Y, Sheng Y, Yue G. 2016. Response of hydrological processes to permafrost degradation from 1980 to 2009 in the upper Yellow river basin, China. *Hydrology Research* 47(5).

Qin Y, Yang D, Gao B, Wang T, Chen J, Chen Y, Wang YH, Zheng GH. 2017. Impacts of climate warming on the frozen ground and eco-hydrology in the Yellow river source region, china. *Science of the Total Environment* 605-606: 830.

Qiao B, Zhu L. 2017. Differences and cause analysis of changes in lakes of different supply types in the north-western Tibetan Plateau. *Hydrological Processes* 31(15): 2752-2763.

Rodell MP, Houser U, Jambor J, Gottschalck K, Mitchell CJ, Meng K, Arsenault B, Cosgrove J, Radakovich M, Bosilovich JK, Entin JP, Walker D, Lohmann D. 2004. The Global Land Data Assimilation System. *Bulletin of the American Meteorological society* 85 (3): 381-394.

Rodell M, Famiglietti JS, Chen J, Seneviratne SI, Viterbo P, Holl S, Wilson CR. 2004. Basin scale estimates of evapotranspiration using GRACE and other observations. *Geophysical Research Letters* 31 (20): 183-213.

Rodell M, Velicogna I, Famiglietti J. 2009. Satellite-based estimates of groundwater depletion in India. *Nature* 460: 999-1002.

Shen YP, Xie ZC, Ding LF, Liu JS. 1997. Estimation of average mass balance for glacier in a watershed and its application. *Journal of Glaciology and Geocryology* 19: 302-307.

Smith M. 2000.The application of climatic data for planning and management of sustainable rainfed and irrigated crop production. *Agricultural and Forest Meteorology* 103: 99-108.

Shen YP, Liu SY, Zhen LL, Wang GX, Liu GS, 2001. Fluctuations of glacier mass balance in watersheds of Qilian Mountain and their impact on water resources of Hexi Region. *Journal of Glaciology and Geocryology* 23: 244 -250.

Swenson SC, Wahr J. 2006. Post-processing removal of correlated errors in GRACE data. *Geophysical Research Letters* 33: L08402.

Swenson SC, Chambers DP, Wahr J. 2008. Estimating geocenter variations from a combination of GRACE and ocean model output. *Journal of Geophysical Research* 113 (B8) : 194-205.

Syed TH, Famiglietti JS, Rodell M, Chen J, Wilson CR. 2008. Analysis of terrestrial water storage changes from GRACE and GLDAS. *Water Resources Research* 44 (2): W02433.

Stahl K, Moore RD, Shea JM, Hutchinson D, Cannon, AJ. 2008. Coupled modelling of glacier and streamflow response to future climate scenarios. *Water Resources Research*, 440(2): 187-194.

Sheng, Y., Li, J., Wu, J. C., Ye, B. S., Wang, J. 2010. Distribution patterns of permafrost in the upper area of Shule river with the application of GIS technique. *Journal of China University of Mining and Technology* 39(1): 32-39.

Strassberg G, Scanlon BR, Rodell M. 2014. Comparison of seasonal terrestrial water storage variations from GRACE with groundwater-level measurements from the high plains aquifer (USA). *Geophysical Research Letters* 34 (14).

Smith LC, Pavelsky TM, Macdonald GM, Shiklomanov AI, Lammers RB. 2007. Rising minimum daily flows in northern eurasian rivers: a growing influence of groundwater in the high-latitude hydrologic cycle. *Journal of Geophysical Research* 112(G4): 10-1029.

Sorg A, Huss M, Rohrer M, Stoffel M. 2014. The days of plenty might soon be over in glacierized central asian catchments. *Environmental Research Letters*, 9(10): 104018.

Su F, Zhang L, Ou T, Chen D, Yao T, Tong K, Qi Y. 2016. Hydrological response to future climate changes for the major upstream river basins in the tibetan plateau. *Global & Planetary Change*, 136: 82-95.

Woo MK, Yang Z, Xia Z, Yang D. 1994. Streamflow processes in an alpine permafrost catchment, tianshan,

china. *Permafrost and Periglacial Processes* 5(2): 71-85.

Wu Q, Zhang T. 2008. Recent permafrost warming on the Qinghai-Tibetan Plateau. *Journal of Geophysical Research* 113(D13): 3614-3614.

Wang B, Bao Q, Hoskins B, Wu G, Liu Y. 2008. Tibetan plateau warming and precipitation changes in east Asia. *Geophysical Research Letters* 35(14): 63-72.

Wang G, Hu H, Li T. 2009. The influence of freeze-thaw cycles of active soil layer on surface runoff in a permafrost watershed. *Journal of Hydrology* 375(3): 438-449.

Wang G, Liu G, Liu L. 2012. Spatial scale effect on seasonal streamflows in permafrost catchments on the Qinghai-Tibet plateau. *Hydrological Processes* 26(7): 973-984.

Wang G, Mao T, Chang J, Song C, Huang K. 2017. Processes of runoff generation operating during the spring and autumn seasons in a permafrost catchment on semi-arid plateaus. *Journal of Hydrology* 550: 307-317.

Xiao R, He X, Zhang Y, Ferreira VG, Chang L. 2015. Monitoring groundwater variations from satellite gravimetry and hydrological models: a comparison with in-situ measurements in the mid-Atlantic region of the united states. *Remote Sensing* 7(1): 686-703.

Yao, T., Wang, Y., Liu, S., Pu, J., Shen, Y., Lu, A. 2004. Recent glacial retreat in High Asia in China and its impact onwater resource in Northwest China. *Science in China* 47 (12): 1065-1075.

Ye B, Yang D, Jiao K, Han T, Jin Z, Yang H, Li ZQ. 2005. The urumqi river source glacier no. 1, Tianshan, China: changes over the past 45 years. *Geophysical Research Letters* 32(21): 154-164.

Yao J, Zhao L, Ding Y, Gu L, Jiao K, Qiao Y, Wang X. 2008. The surface energy budget and evapotranspiration in the Tanggula region on the Tibetan Plateau. *Cold Regions Science and Technology* 52(3): 326-340.

Ye B, Yang D, Zhang Z, Kane DL. 2009. Variation of hydrological regime with permafrost coverage over Lena basin in Siberia. *Journal of Geophysical Research* 114(D7): 1291-1298.

Yi S, Zhou Z, Ren S, Xu M, Qin Y, Chen S, Ye B. 2011. Effects of permafrost degradation on alpine

grassland in a semi-arid basin on the Qinghai-Tibetan Plateau. *Environmental Research Letters* 6(4): 45403-45409.

Yang K, Zhou D, Wu B, Foken T, Qin J, Zhou Z. 2011. Response of hydrological cycle to recent climate changes in the Tibetan Plateau. *Climate Change* 109(3-4): 517-534.

Yao T, Thompson LG, Yang W, Yu W, Gao Y, Guo X, Yang X, Duan K, Zhao H, Xu B, Pu J, Lu A, Xiang Y, Kattel D, Joswiak D. 2012. Different glacier status with atmospheric circulations in Tibetan Plateau and surroundings. *Nature Climate Change* 2: 663-667.

Yao TD, Qin DH, Shen YP, Zhao L, Wang NL. 2013. Cryospheric changes and their impacts on regional water cycle and ecological conditions in the Qinghai Tibetan Plateau. *Chinese Journal of Nature* 35: 179-186.

Yang T, Wang C, Yu Z, Xu F. 2013. Characterization of spatio-temporal patterns for various grace- and gldas-born estimates for changes of global terrestrial water storage. *Global & Planetary Change* 109(4): 30-37.

Yang K, Wu H, Qin J, Lin C, Tang W, Chen Y. 2014. Recent climate changes over the Tibetan Plateau and their impacts on energy and water cycle: A review. *Global & Planetary Change* 112: 79-91.

Zhang YQ, Liu CM, Tang YH, Yang YH. 2007. Trends in pan evaporation and reference and actual evapotranspiration across the Tibetan Plateau. *Journal of Geophysical Research* 112(D12): 113-120.

Zhang Y, Chen W, Riseborough DW. 2008. Transient projections of permafrost distribution in Canada during the 21st century under scenarios of climate change. *Global & Planetary Change* 60(3): 443-456.

Zhu BW. 2008. Some characteristic analysis on surface runoff of alpine meadow grassland. *Journal of Anhui Agricultural Sciences* 36(13): 5588-5590.

Zhang SQ, Gao X, Ye BS, Zhang XW, Hagemann S. 2012. A modified monthly degree-day model for evaluating glacier runoff changes in China. Part II: Application. *Hydrological Processes* 26: 1697–1706.

Zhang W, Yi Y, Song K, Kimball J, Lu Q. 2016. Hydrological response of alpine wetlands to climate warming in the eastern Tibetan Plateau. *Remote Sensing* 8(4): 336.

Zhang C, Shen Y, Liu F, Meng L. 2016. Changes in reference evapotranspiration over an agricultural region in the qinghai-tibetan plateau, china. *Theoretical & Applied Climatology*, 123(1-2): 107-115.

Tab. 1 Mann-Kendall test on monotonic trend for air temperature during 1957-2010

	Z_c	β	H_0
Annual	5.83	0.034	R
Spring	2.65	0.020	R
Summer	3.94	0.027	R
Autumn	4.73	0.039	R
Winter	4.57	0.062	R

*R: rejected; A: accepted.

Tab. 2 Mann-Kendall test on monotonic trend for precipitation during 1957-2010

	Z_c	β	H_0
Annual	2.69	1.35	R
Spring	-0.06	-0.0057	A
Summer	3.28	1.12	R
Autumn	2.09	0.39	R
Winter	0.57	0.0098	A

*R: rejected; A: accepted.

Tab. 3 Mann-Kendall test on monotonic trend for discharge

	Z_c	β	H_0
Annual (1957-2010)	4.22	0.079	R
Spring (1970-2006)	2.28	0.0074	R
Summer (1970-2006)	2.05	0.052	R
Fall (1970-2006)	2.26	0.013	R
Winter (1970-2006)	2.89	0.0077	R

*R: rejected; A: accepted.

Tab. 4 Variations in annual discharge and glacier discharge in different periods

	Total discharge (10^8 m^3)	Glacier discharge (10^8 m^3)	Percentage of glacier discharge (%)
1950s	8.45	2.83	33.6
1960s	8.03	2.54	30.9
1970s	8.91	2.99	31.4
1980s	9.23	2.69	28.5
1990s	8.97	3.23	35.6
2000s	12.81	5.90	44.7

Tab. 5 Mann-Kendall test on monotonic trend for ET during 1957-2010

	Z_c	β	H_0
Annual	4.92	1.34	R
Spring	1.55	0.083	A
Summer	5.16	0.97	R
Autumn	4.02	0.27	R
Winter	1.13	0.013	A

*R: rejected; A: accepted.

Tab. 6 Changes in precipitation, temperature, glacier mass balance, glacier discharge and total discharge between 1957-1994 and 1995–2010 in the study area

	P (mm)	T (℃)	Glacier mass balance (mm)	R_{gd} (mm)	$Discharge_g$ (10^8 m^3)	Total discharge (10^8 m^3)
1957-1994	285.2	-2.97	-7.3	24.8	2.71	8.49
1995-2010	312.3	-1.82	-193.2	48.4	5.31	11.81
Change	27.1	1.15	-185.9	23.6	2.60	3.32
Change (%)	9.5			95.2	95.2	39.6

*R_{gd} and $Discharge_g$ are the depth and the volume of glacier runoff, respectively.

Tab. 7 Relationships(R) between temperature and GRACE-derived total water storage change and soil water content change modeled by GLDAS

		T_{annual}	T_{spring}	T_{summer}	T_{autumn}	T_{winter}
Annual	ΔW_{GRACE}	-0.51*	0.60*	-0.80*	0.12	-0.56*
Annual	ΔW_{GLDAS}	0.19	-0.13	-0.02	0.59*	-0.37*

*p<0.05

Tab. 8 Relationships(R) between precipitation and GRACE-derived total water storage change and soil water content change modeled by GLDAS

		P_{annual}	P_{spring}	P_{summer}	P_{autumn}	P_{winter}
Annual	ΔW_{GRACE}	-0.20	-0.37*	0.01	-0.24	0.47*
Annual	ΔW_{GLDAS}	0.27	-0.41*	0.31*	0.68*	0.68*

*p<0.05

Tab. 9 Regression analysis of the dependence of discharge on temperature and precipitation in the study area

	Equation	R^2	Standard error of estimate	p
(1)	Q=22.305T-101.452	0.468	16.78	P<0.01
(2)	Q=0.263P+10.249	0.388	17.96	P<0.01
(3)	Q=0.208P+18.626T-113.053	0.695	13.78	P<0.01
(4)	$Q=e^{-2.50873}*P^{0.704003}*T^{1.47456}$	0.708	12.52	P<0.01

Tab. 10 Changes in temperature (Δ T) and precipitation (Δ P) for the climate sensitivity tests of runoff (unit: mm) in the study area

	Δ P+20%	Δ P+10%	Δ P+5%	Δ P	Δ P-5%	Δ P-10%	Δ P-20%
Δ T	11.12	5.26	2.27	0	-3.83	-6.96	-13.37
Δ T+0.5℃	20.91	14.47	11.17	7.86	4.47	1.04	-6.00
Δ T+1℃	31.00	23.96	20.37	16.73	13.03	9.28	1.58
Δ T+2℃	52.03	43.75	39.52	35.23	30.88	26.46	17.39

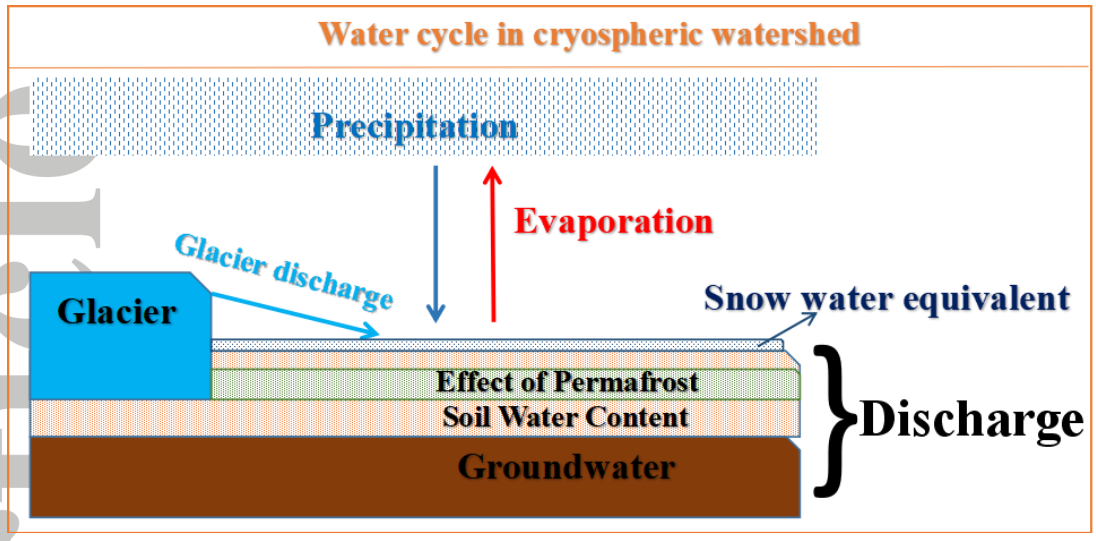

Fig. 1 The different components of the water balance in the cryospheric watershed

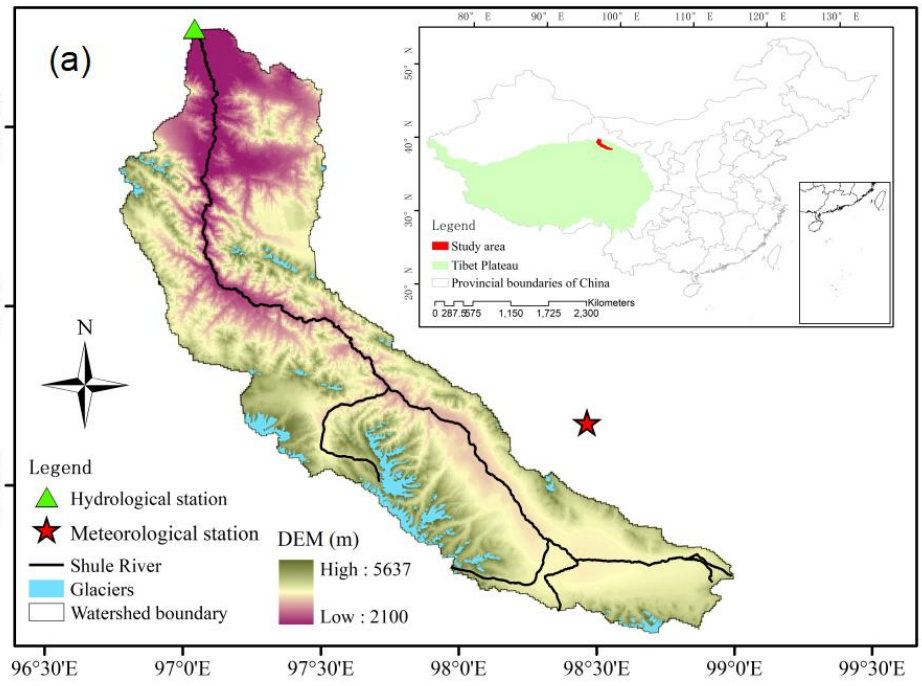

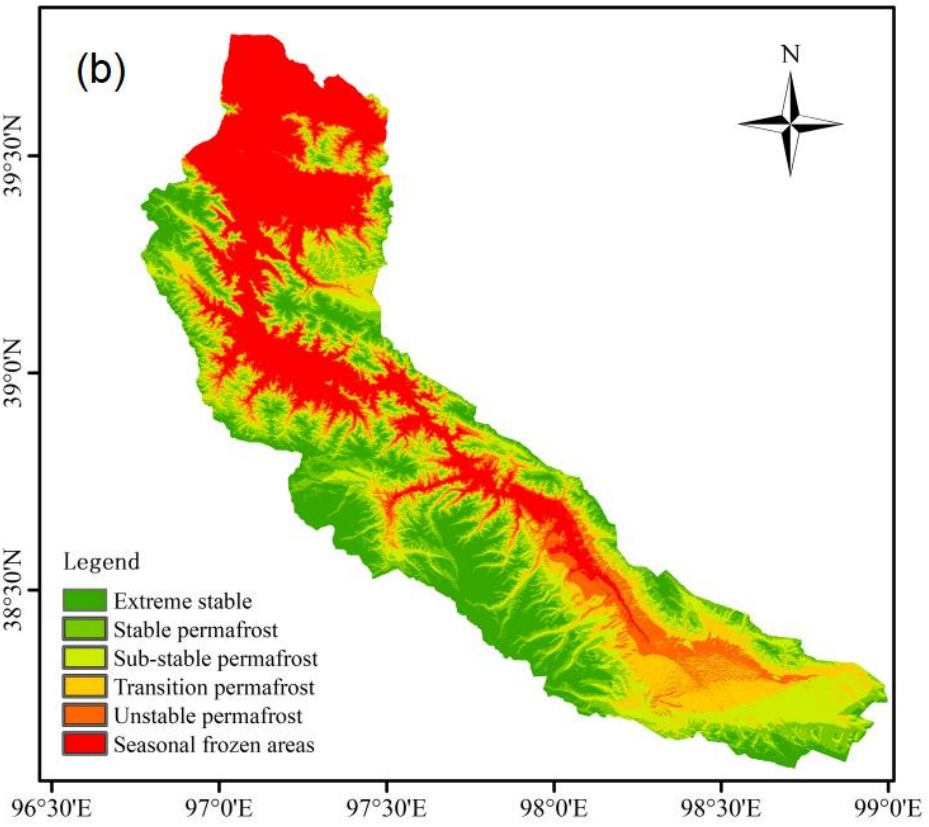

Fig. 2 Location of upstream of Shule River Basin (a) and spatial distribution of frozen soil in the upstream

of Shule River Basin (b)

Fig. 3 Observations of discharge ratio in sub-watersheds of study area

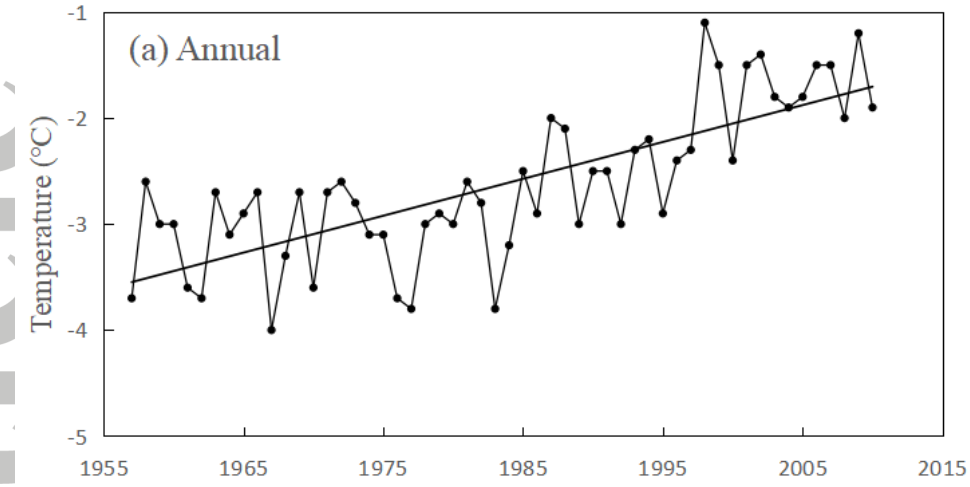

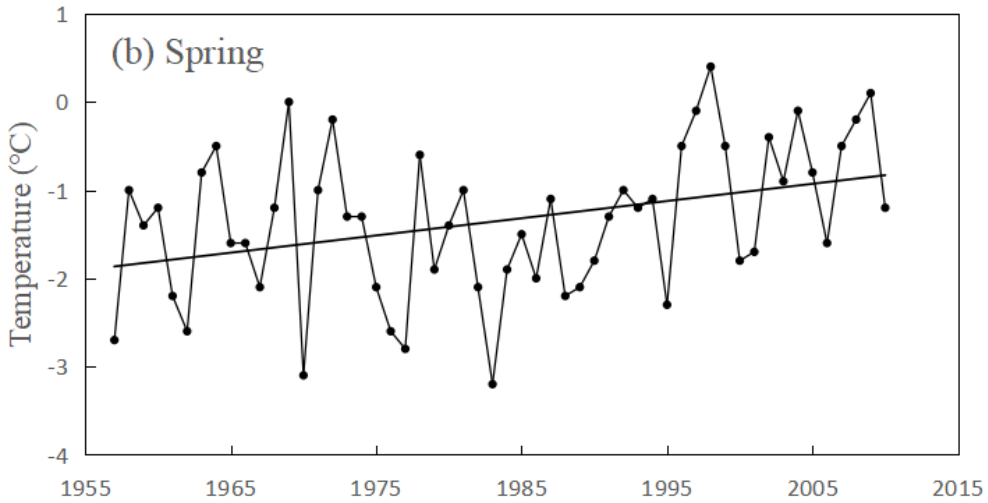

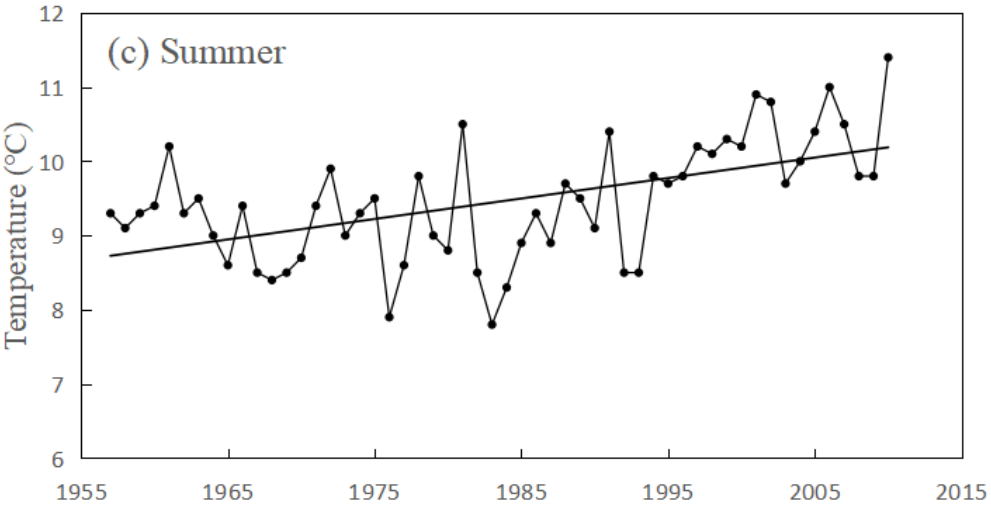

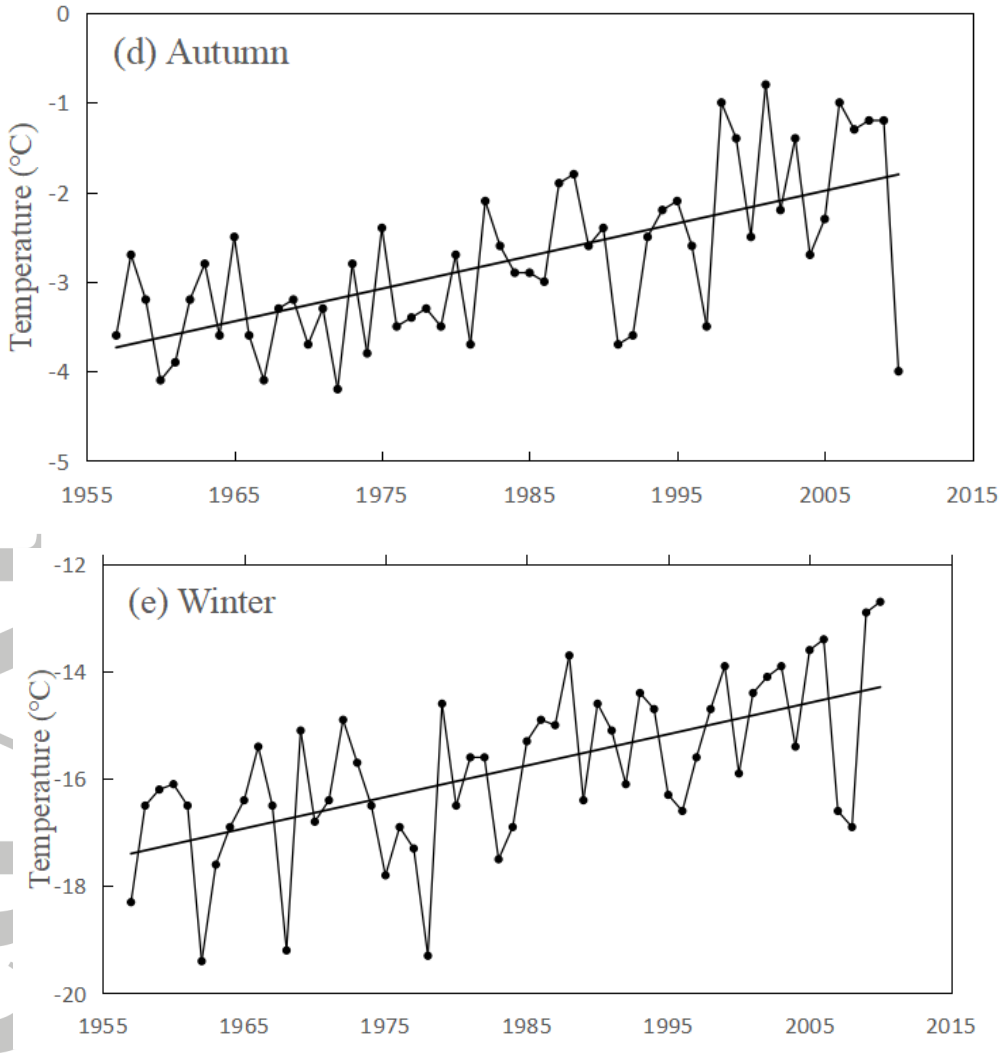

Fig. 4 (a) Mean annual air temperature, (b-e) seasonal mean air temperature in the Tuole station during 1957-2010

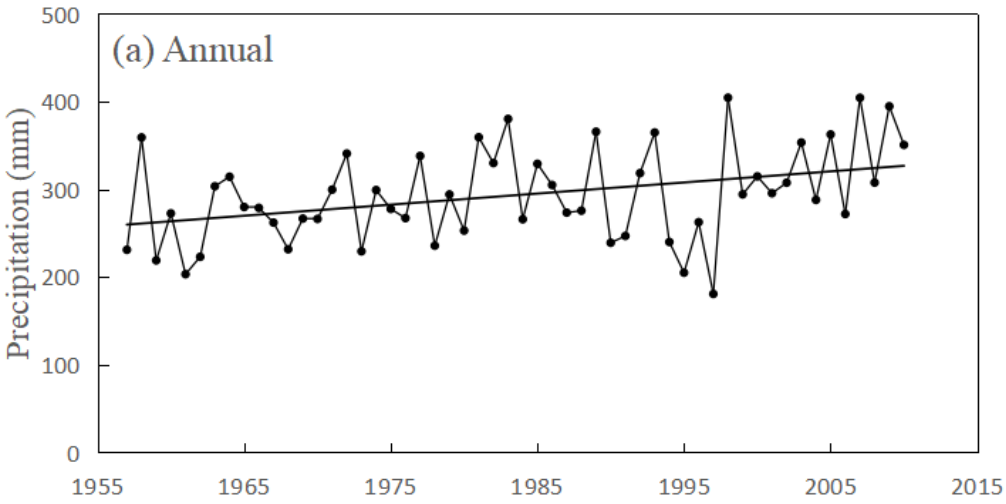

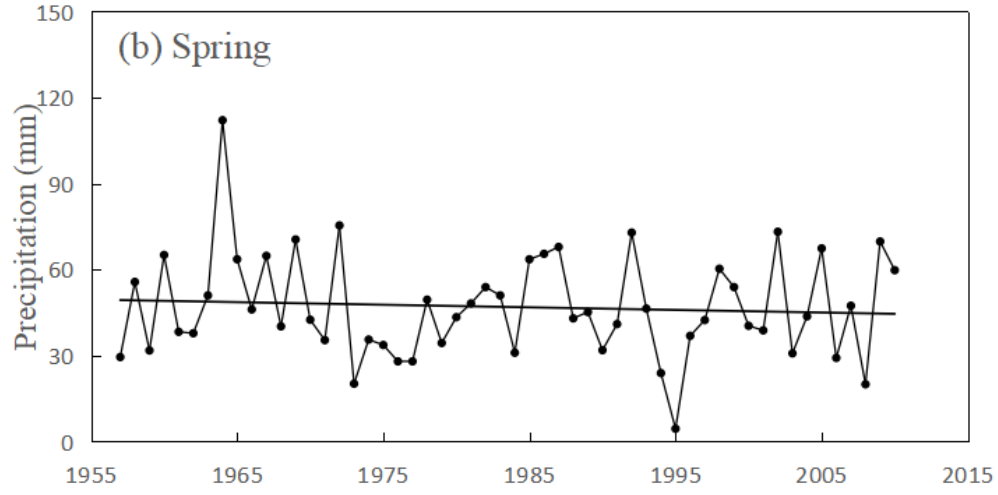

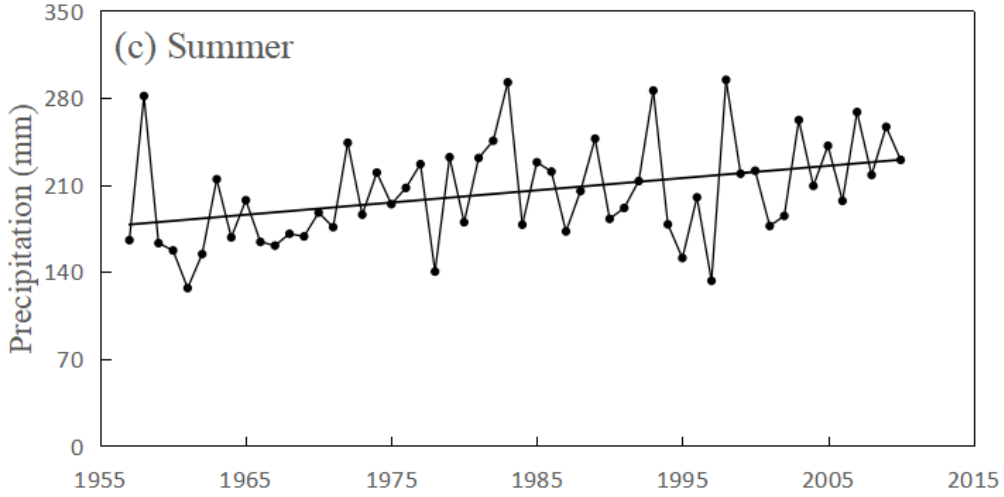

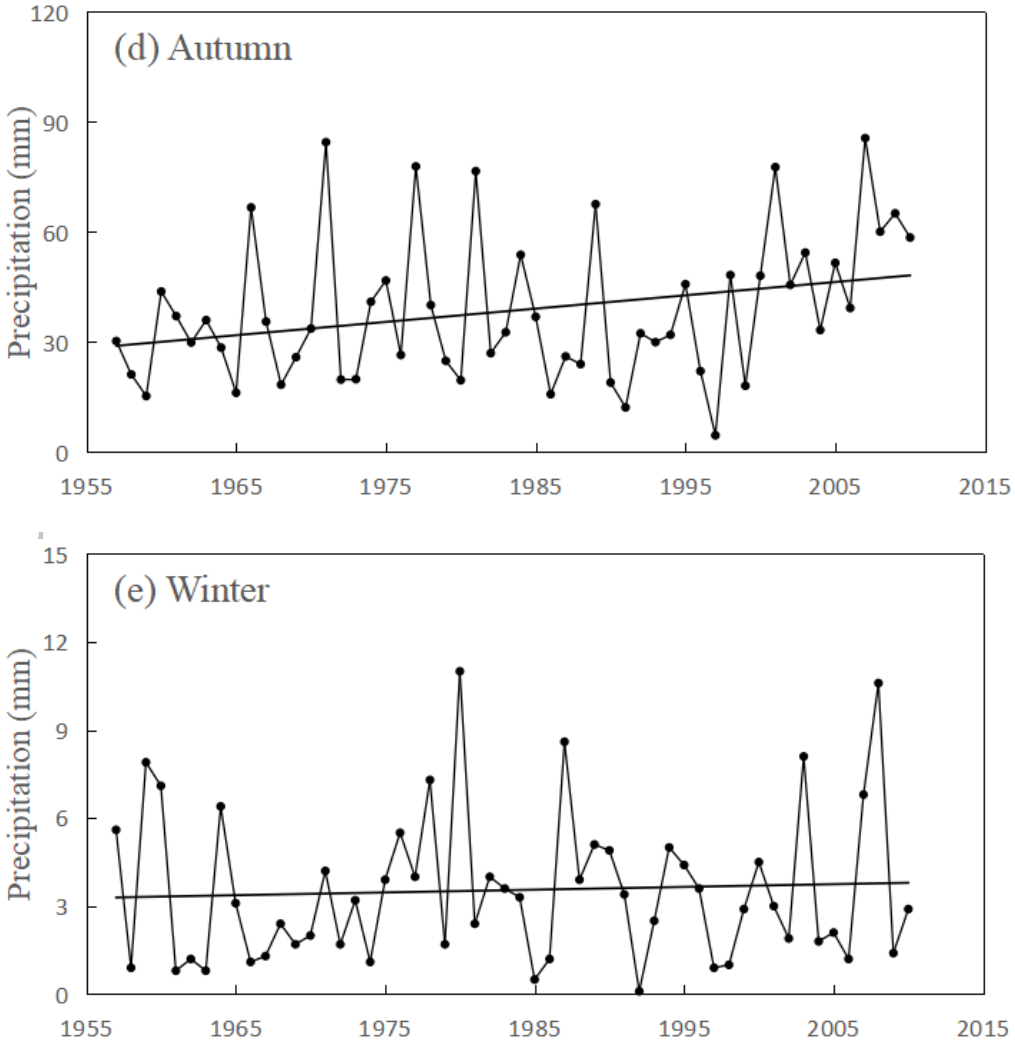

Fig. 5 (a) annual precipitation, (b-e) seasonal precipitation in the Tuole station during 1957-2010

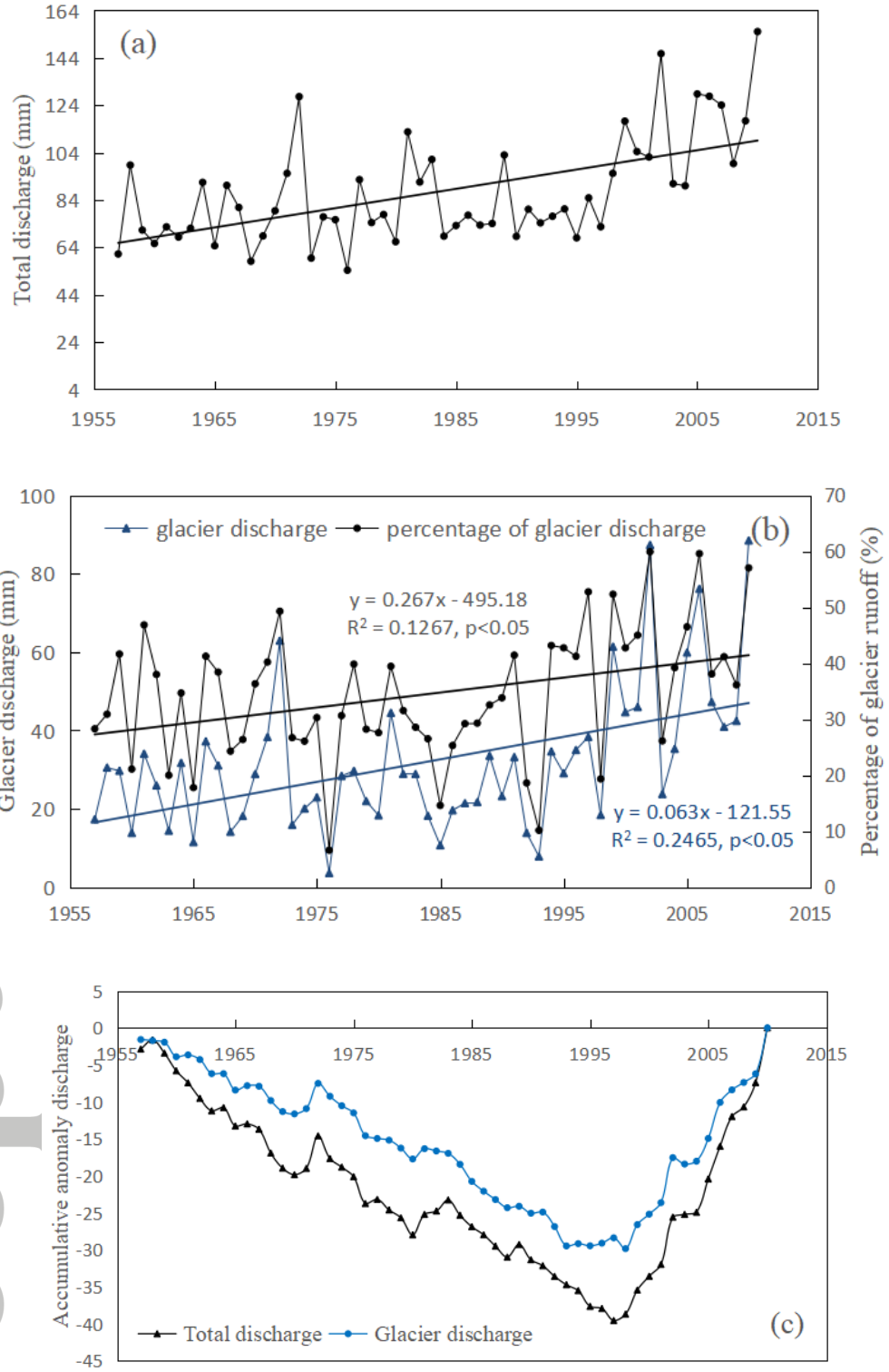

Fig. 6 (a) Variations in annual discharge, (b) glacier discharge and the contribution of glacier discharge to total discharge and (c) cumulative annual discharge and glacier discharge in the upstream of Shule River Basin during 1957-2010

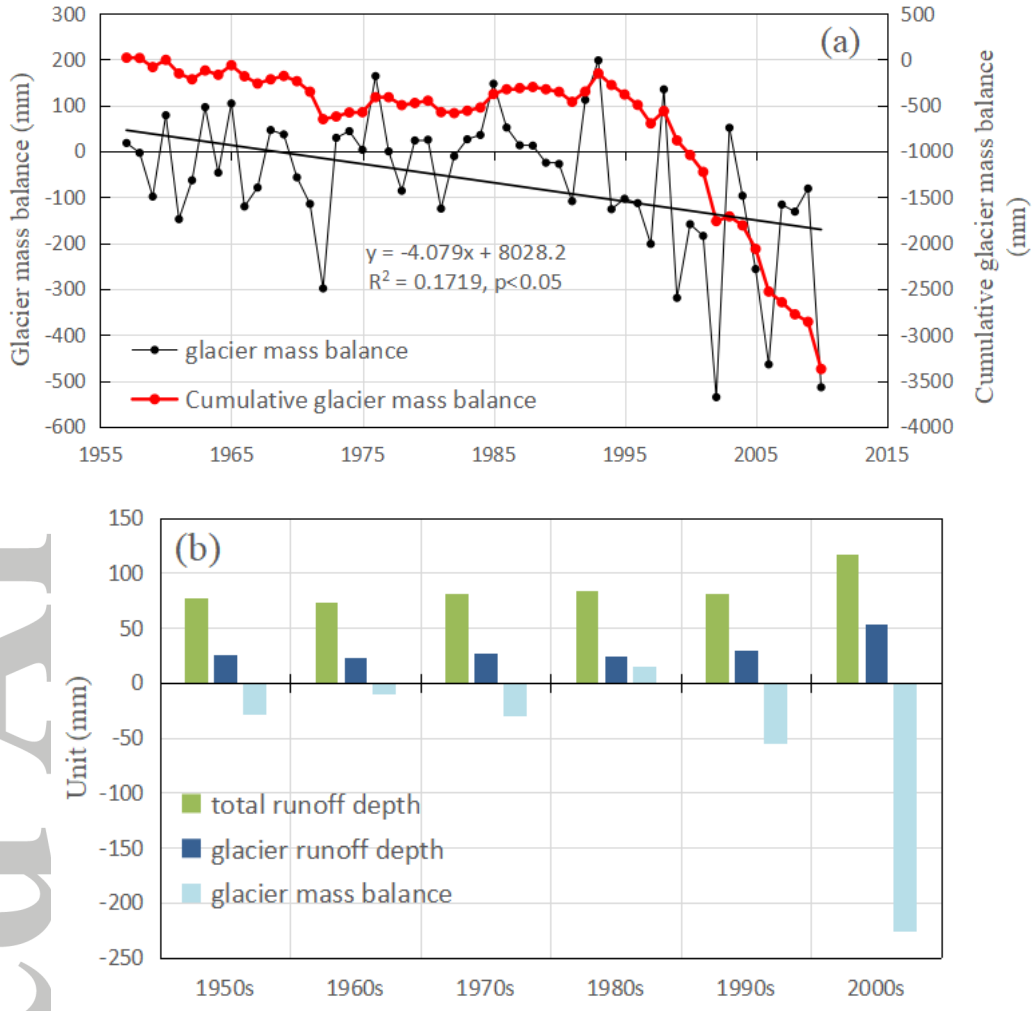

Fig. 7 (a) Variations of glacier mass balance and cumulative glacier mass balance, (b) Variations of total runoff depth, glacier runoff depth and glacier mass balance in the upstream of Shule River Basin during 1957-2010

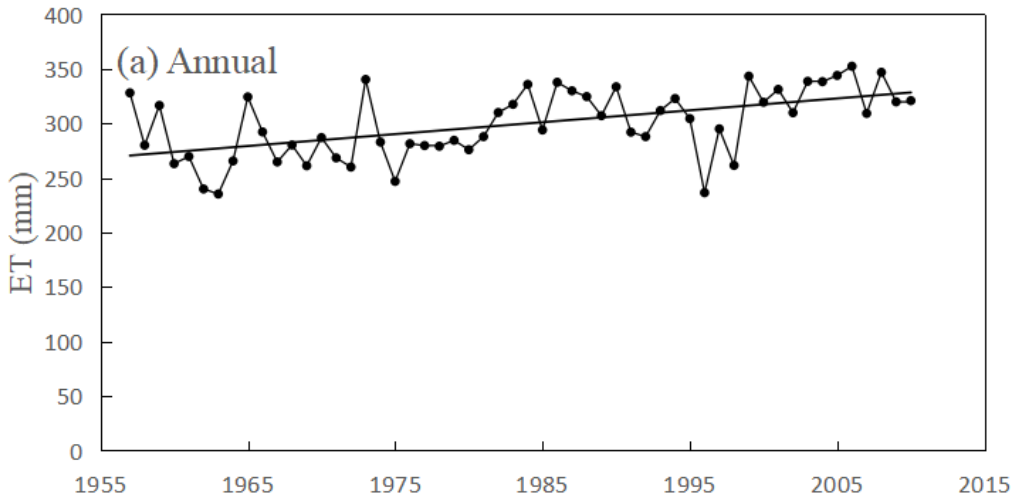

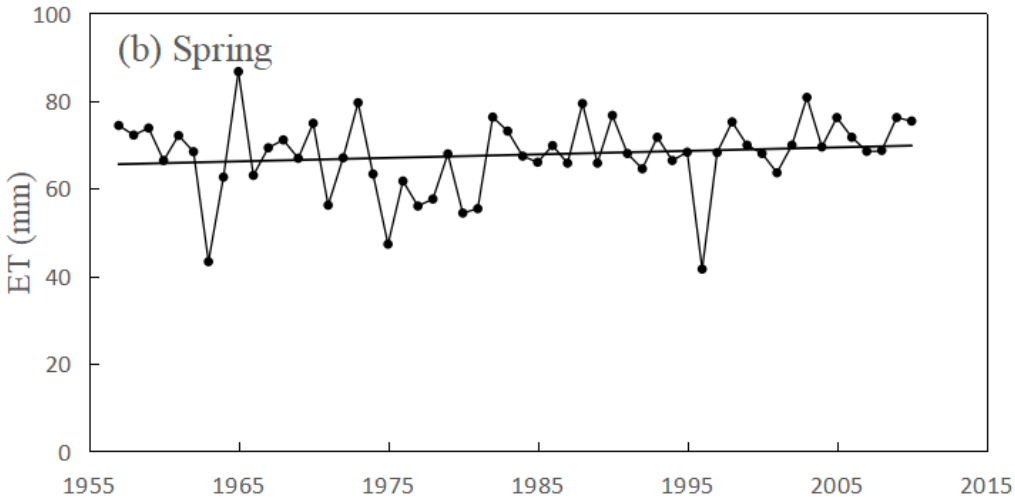

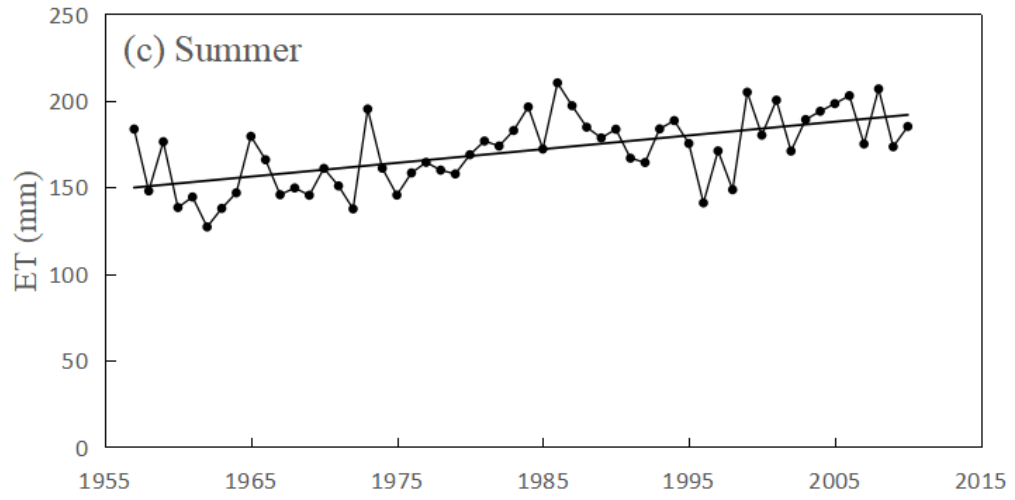

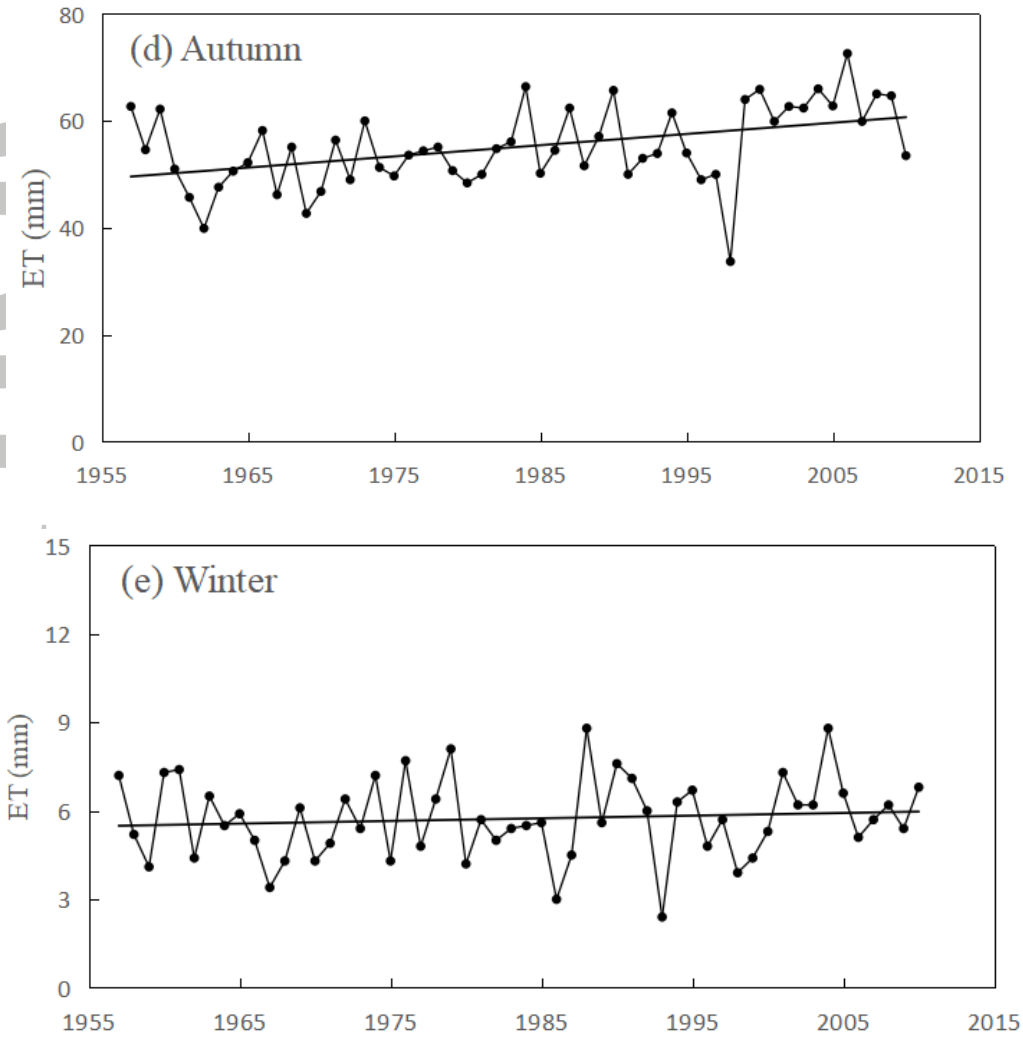

Fig. 8 Variations of (a) annual ET and (b-e) seasonal ET in the Tuole station during 1957-2010

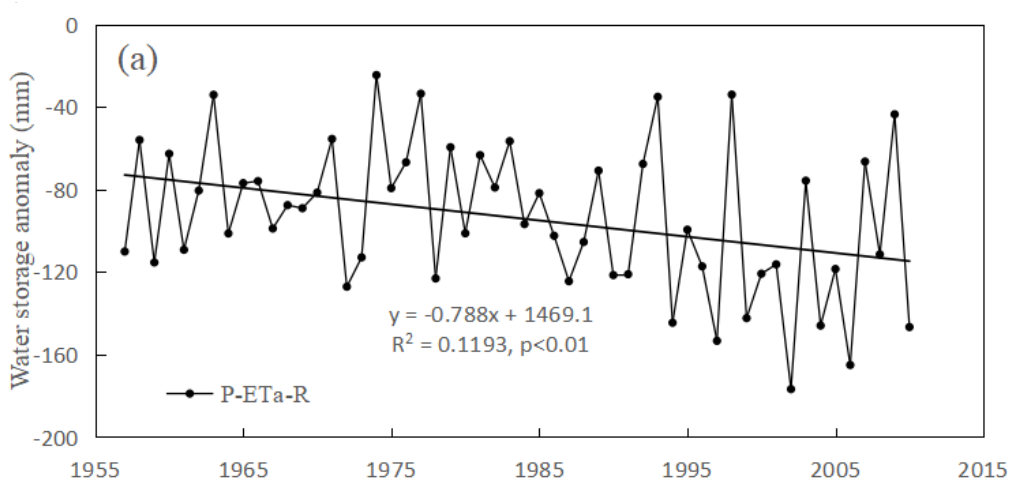

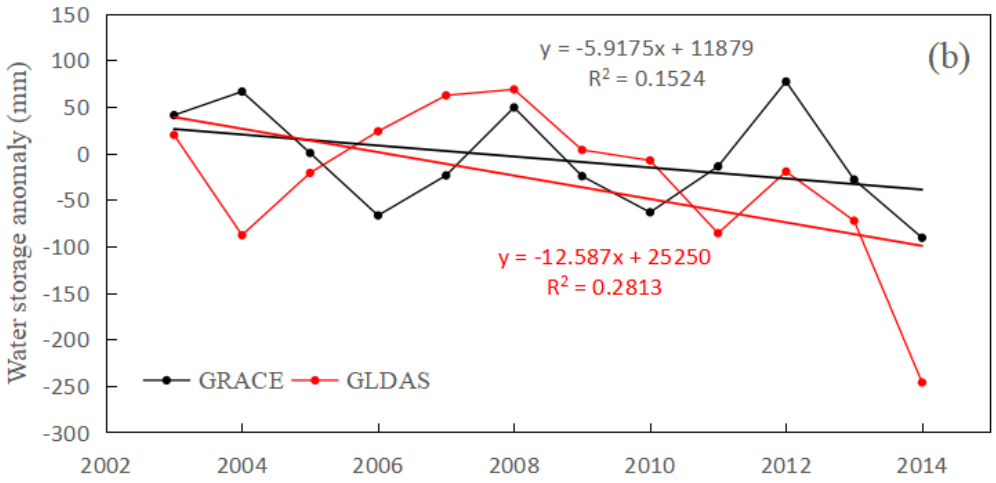

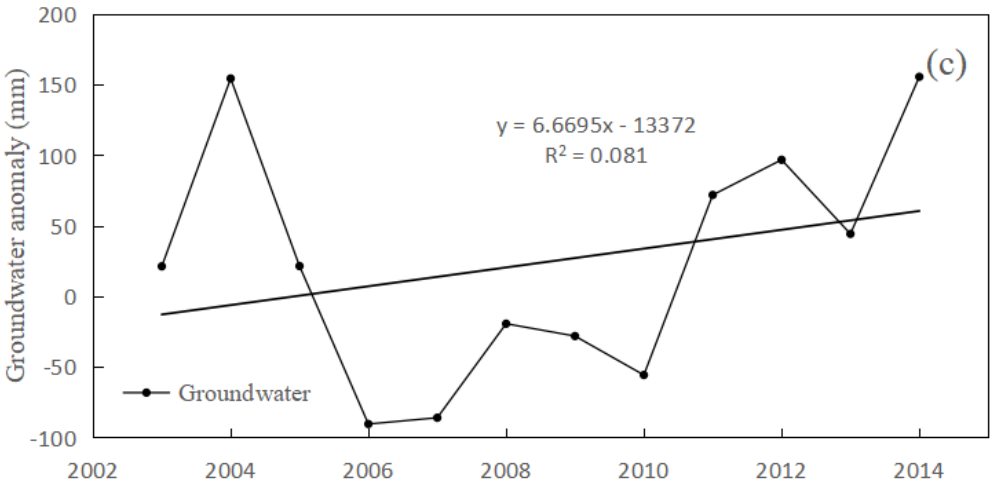

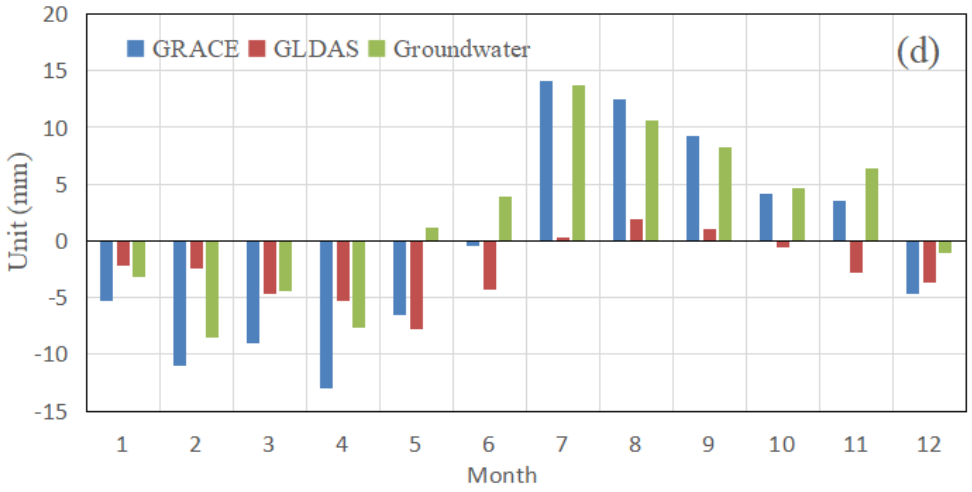

Fig. 9 (a) Total water storage change anomaly calculated by water balance during 1957-2010 in the study area, (b) Total water storage change retrieved by GRACE and soil water content change modeled by GLDAS, (c) Groundwater storage change estimated from GRACE and GLDAS data, (d) Monthly distribution of total water storage change retrieved by GRACE, soil water content change modeled by GLDAS and Groundwater change

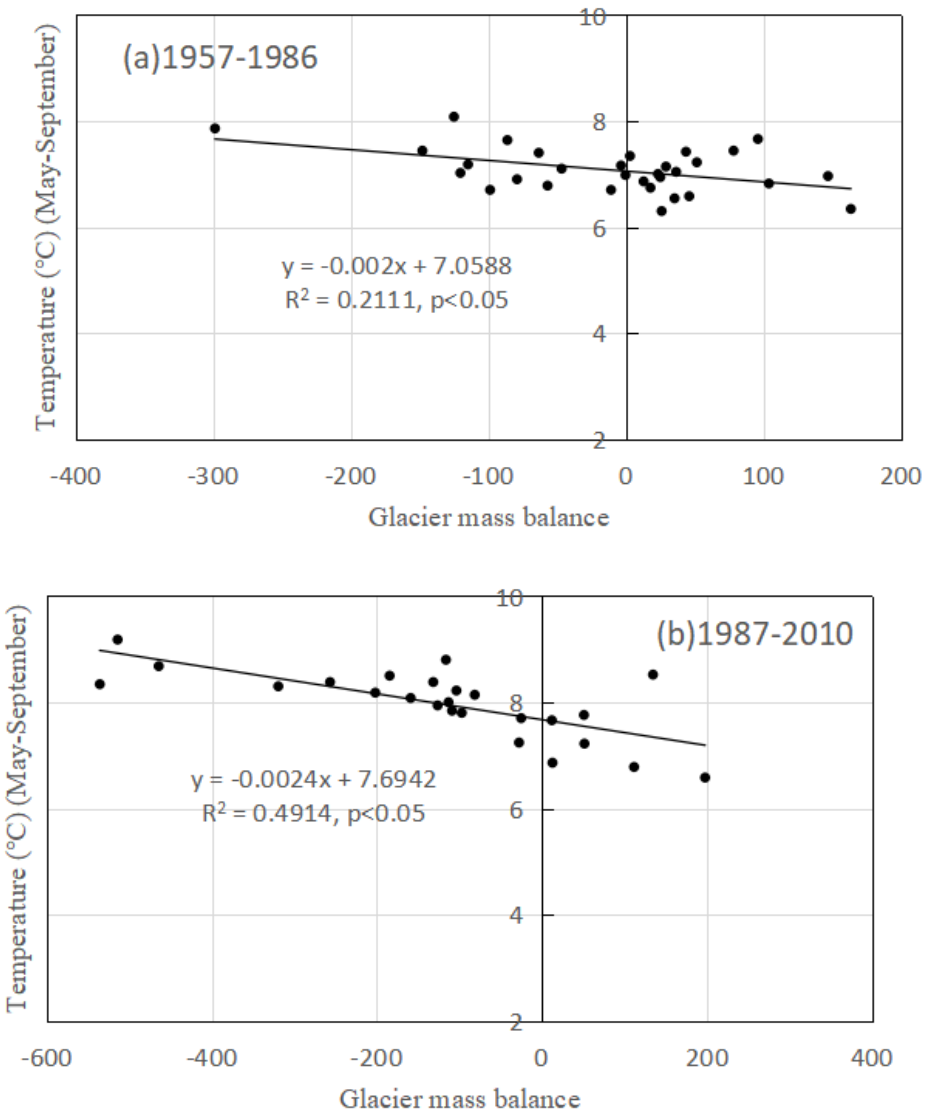

Fig. 10 The relationship between glacier mass balance and temperature during (a) 1957-1986 and (b) 1987-2010

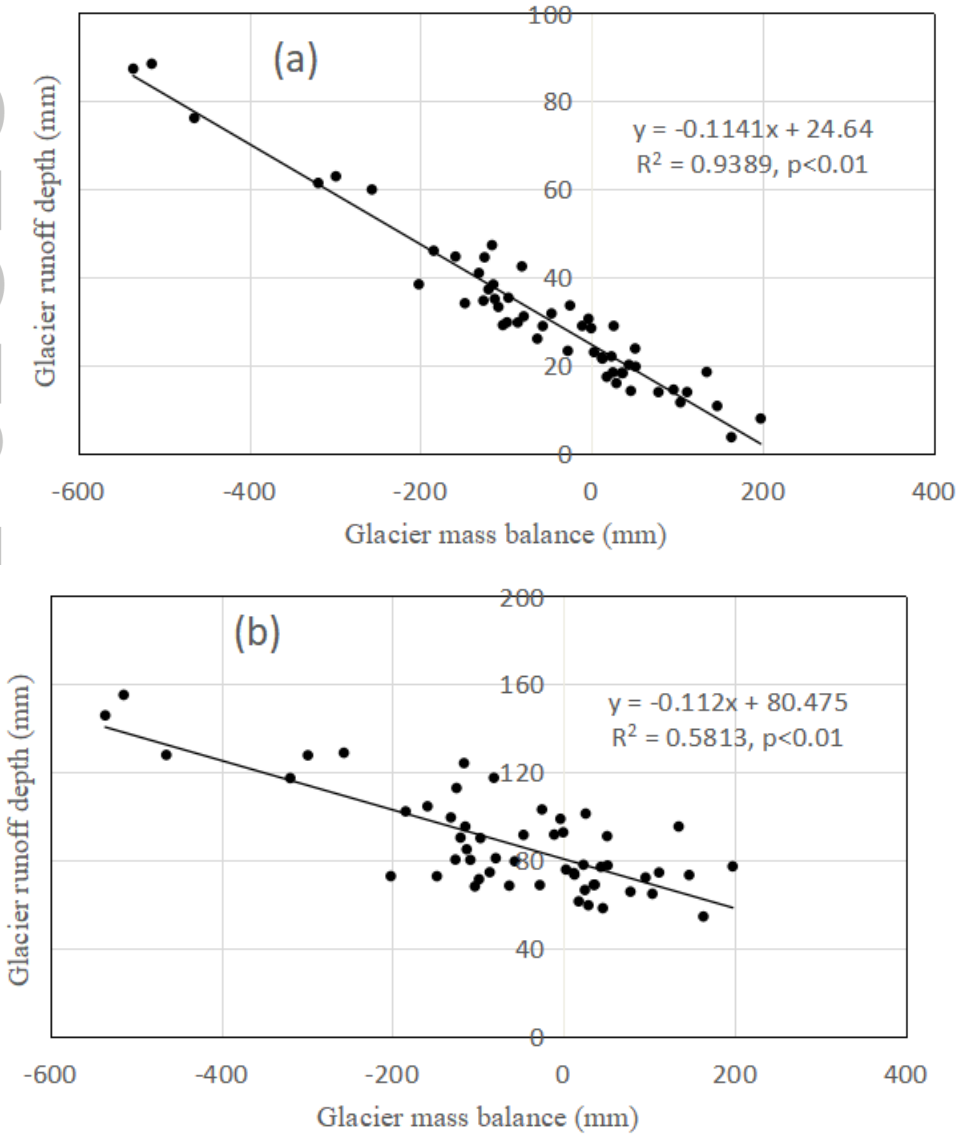

Fig. 11 The relationship between glacier discharge and glacier mass balance in the study area.

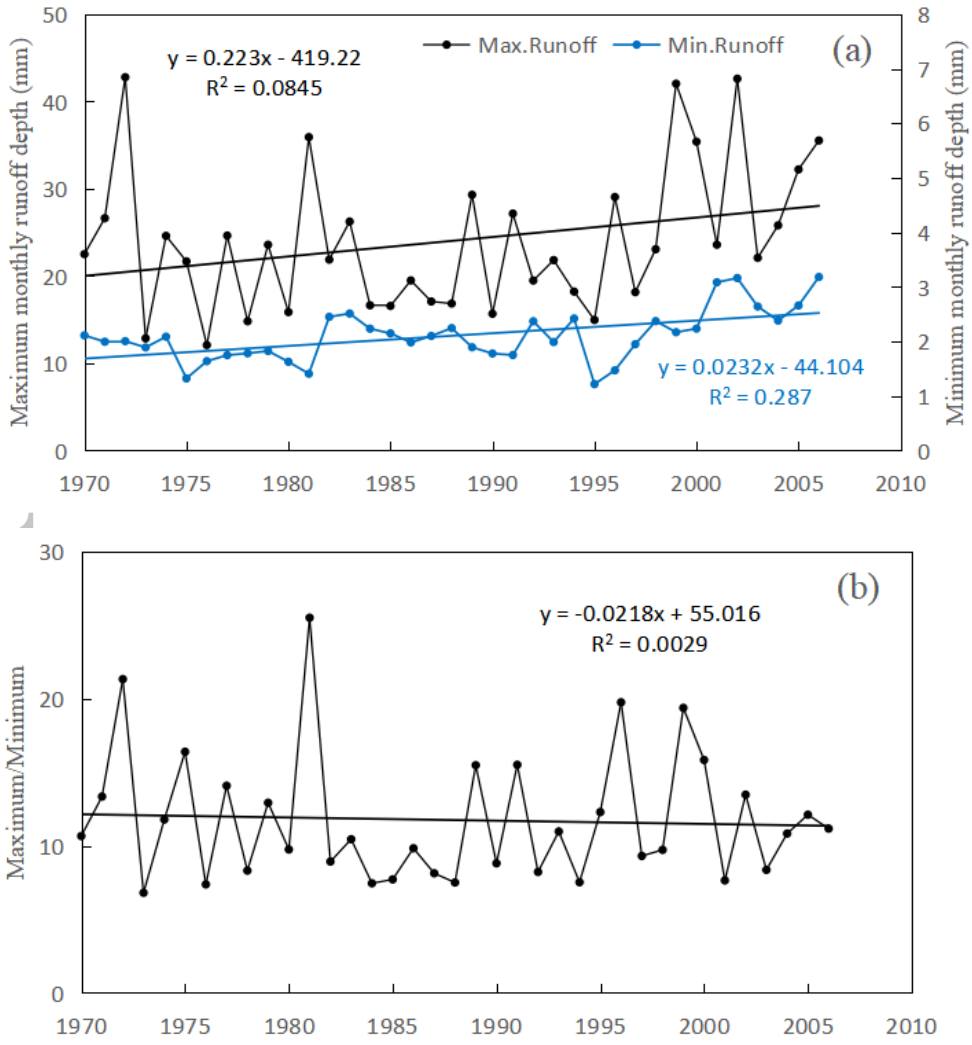

Fig. 12 Maximum depth of runoff (R_{max}), minimum depth of runoff (R_{min}), and ratio of R_{max}/R_{min} in the study area during 1979 – 2006.

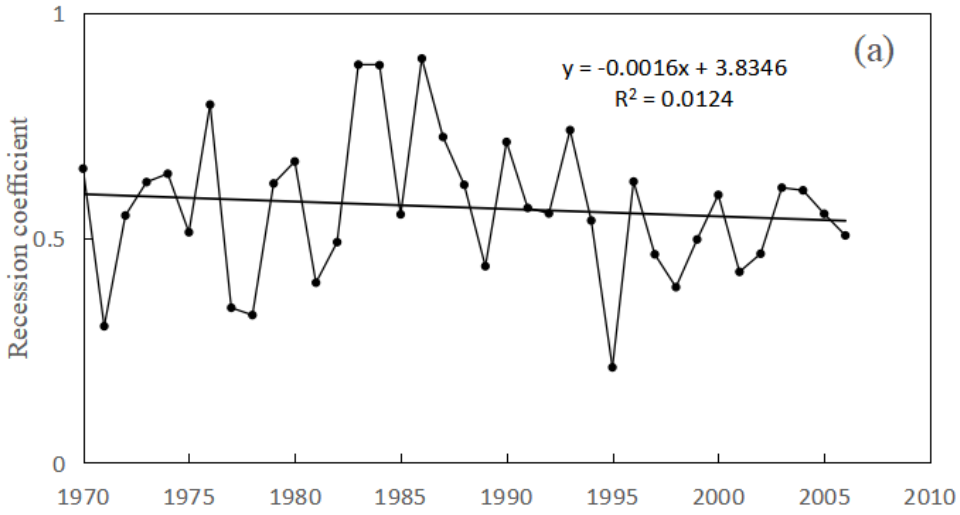

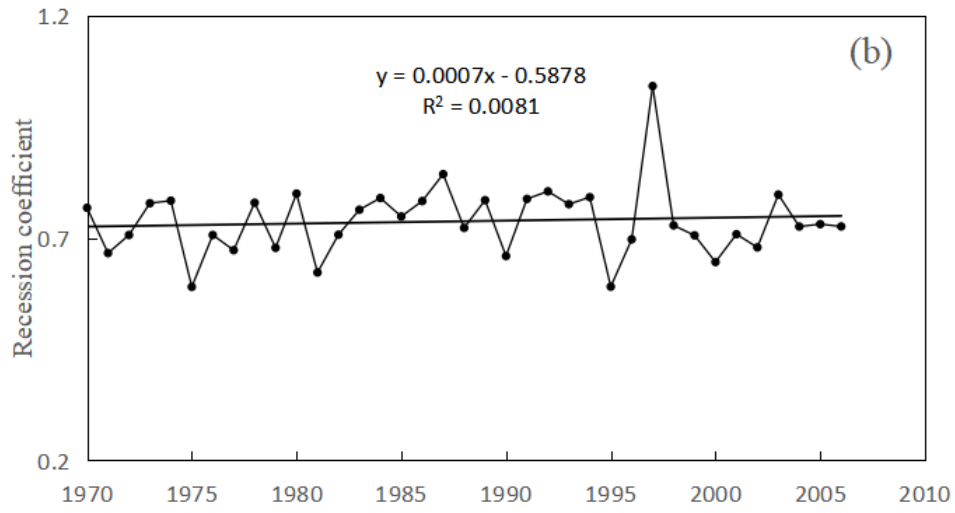

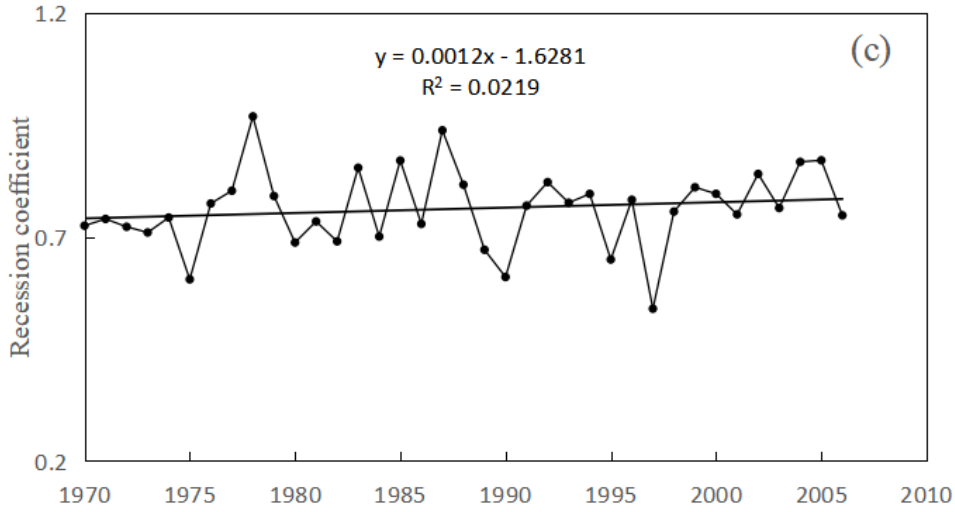

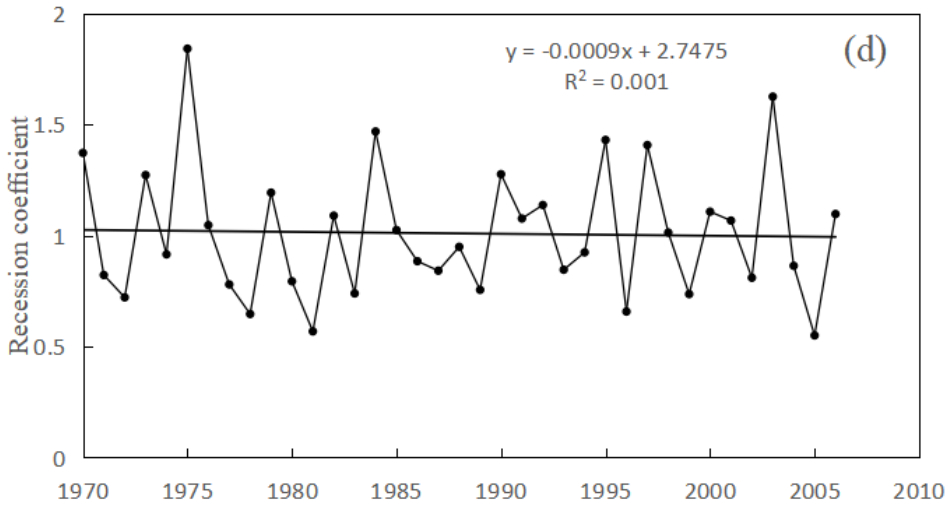

Fig. 13 Monthly recession coefficient (RC) of discharge in the study area during 1970-2006

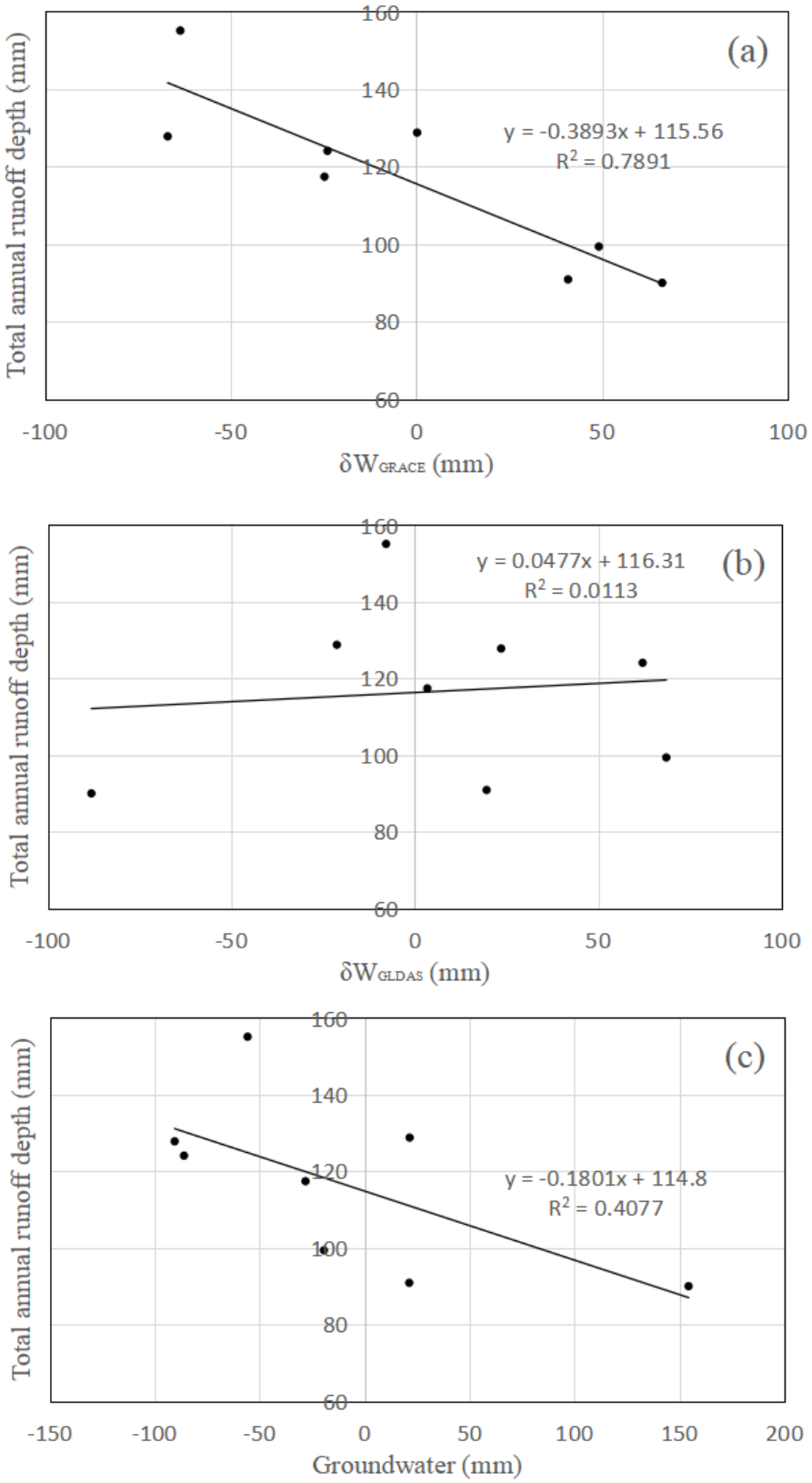

Fig. 14 Relationships between (a) total runoff and GRACE-derived total water storage change, (b) total runoff and soil water content modeled by GLDAS, (c) total runoff and groundwater

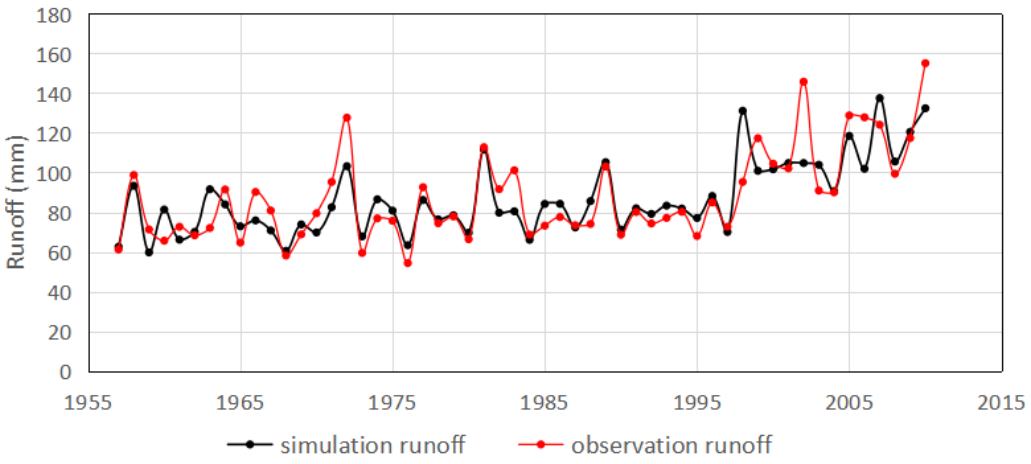

Figure 15 Comparison of the results of nonlinear regression and observation